


RESEARCH

Open Access



Silicon-induced mitigation of salt stress in GF677 and GN15 rootstocks: insights into physiological, biochemical, and molecular mechanisms

Pouya Gharbi¹, Jafar Amiri^{1*} , Nasser Mahna², Lotfali Naseri¹ and MirHassan Rasouli Sadaghiani³

Abstract

Salinity is a common environmental stress that disrupts physiological and biochemical processes in plants, inhibiting growth. Silicon is a key element that enhances plant tolerance to such abiotic stresses. This study examined the effects of silicon supplementation on physiological, biochemical, and molecular responses of GF677 and GN15 rootstocks under NaCl-induced salinity stress. The experiment was conducted in a greenhouse using a factorial design with two rootstocks, three NaCl concentrations (0, 50, and 100 mM), and three silicon levels (0, 1, and 2 mM) in a randomized complete block design with three replicates. Salinity significantly reduced growth parameters, including shoot and root fresh and dry weights, RWC, and photosynthetic activity, with GN15 being more sensitive to salt stress than GF677. Silicon supplementation, especially at 2 mM, alleviated NaCl-induced damage, enhancing biomass retention and RWC under moderate and high NaCl levels. Additionally, silicon reduced electrolyte leakage, lipid peroxidation, and hydrogen peroxide accumulation, suggesting a protective role against oxidative stress. Biochemical analyses showed that silicon increased the accumulation of osmolytes such as proline, soluble sugars, glycine betaine, and total soluble protein, particularly in GF677. Silicon also boosted antioxidant enzyme activities, mitigating oxidative damage. In terms of mineral nutrition, silicon reduced Na⁺ and Cl⁻ accumulation in leaves and roots, with the greatest reduction observed at 2 mM Si. Gene expression analysis indicated that NaCl stress upregulated key salt tolerance genes, including *HKT1*, *AVP1*, *NHX1*, and *SOS1*, with silicon application further enhancing their expression, particularly in GF677. The highest levels of gene expression were found in plants treated with both NaCl and 2 mM Si, suggesting that silicon improves salt tolerance by modulating gene expression. In conclusion, this study demonstrates the potential of silicon as an effective mitigator of NaCl stress in GF677 and GN15 rootstocks, particularly under moderate to high salinity conditions. Silicon supplementation enhances plant growth, osmotic regulation, reduces oxidative damage, and modulates gene expression for salt tolerance. Further research is needed to assess silicon's effectiveness under soil-based conditions and its applicability to other rootstocks and orchard environments. This study is the first to concurrently evaluate

*Correspondence:

Jafar Amiri
jamiri@urmia.ac.ir

Full list of author information is available at the end of the article



© The Author(s) 2025. **Open Access** This article is licensed under a Creative Commons Attribution-NonCommercial-NoDerivatives 4.0 International License, which permits any non-commercial use, sharing, distribution and reproduction in any medium or format, as long as you give appropriate credit to the original author(s) and the source, provide a link to the Creative Commons licence, and indicate if you modified the licensed material. You do not have permission under this licence to share adapted material derived from this article or parts of it. The images or other third party material in this article are included in the article's Creative Commons licence, unless indicated otherwise in a credit line to the material. If material is not included in the article's Creative Commons licence and your intended use is not permitted by statutory regulation or exceeds the permitted use, you will need to obtain permission directly from the copyright holder. To view a copy of this licence, visit <http://creativecommons.org/licenses/by-nc-nd/4.0/>.

the physiological, biochemical, and molecular responses of GF677 and GN15 rootstocks to silicon application under salt stress conditions.

Keywords Antioxidant enzymes, Gene expression, Osmoregulation, Oxidative stress, Silicon, Sodium

Introduction

Soil salinity is a major constraint to agricultural development, currently affecting about 20% of arable land [1]. Secondary salinization results from declining soil organic matter, overuse of fertilizers, poor irrigation practices, reduced rainfall, industrial pollution, and high evaporation rates [2, 3]. If current trends continue, salinization may affect nearly 50% of cultivable land by 2050 [4, 5]. As a major abiotic stressor, salinity disrupts key physiological and biochemical processes, ultimately limiting plant growth and productivity [6].

It impairs water uptake, disturbs water balance, inhibits cell expansion, and reduces stomatal conductance. High levels of sodium (Na^+) and chloride (Cl^-) lead to ionic and oxidative stress, displacing potassium (K^+) in essential biochemical reactions and disrupting protein structure and enzyme function [7, 8]. Plants initially cope with salinity by limiting leaf growth. Under moderate salt stress, root growth is less affected than shoot growth, increasing the root-to-shoot ratio [9]. However, severe salinity inhibits both root and shoot development, leading to significant reductions in dry biomass accumulation [10, 11].

Key genes involved in Na^+ regulation include *SOS1*, *AVP1*, *NHX1*, and *HKT1* [12, 13]. *NHX1* mediates Na^+ sequestration into vacuoles, while *AVP1* encodes a proton pump that supports this process by generating the required electrochemical gradient [14, 15]. *SOS1* expels Na^+ from root cells, and *HKT1* retrieves Na^+ from the xylem, limiting its transport to shoots [16, 17]. Silicon (Si)-containing compounds help mitigate salt stress effects in various horticultural crops. As the second most abundant element in Earth's crust, silicon is present in soils at concentrations between 1% and 45% and accumulates in plant dry matter at levels ranging from 0.1 to 10% [18]. Although not an essential nutrient, silicon offers multiple benefits, especially under stress conditions, by enhancing tolerance and supporting growth [19].

Silicon enhances antioxidant defense systems by boosting enzyme activities that mitigate oxidative stress caused by reactive oxygen species (ROS). It further stabilizes osmotic balance by regulating nutrient uptake and reducing electrolyte leakage, ultimately enhancing plant resilience under salinity stress [20–22].

Silicon also helps maintain osmotic balance, supports key physiological functions, and sustains root biomass under salt stress [23, 24]. It improves nutrient acquisition, increases relative leaf water content, and enhances plant resilience to salinity [25]. Beyond ion regulation,

silicon influences cellular processes such as lignin deposition, chlorophyll synthesis, and hormone regulation, all crucial for stress adaptation. It also modulates polyamine activity, boosts antioxidant enzymes, reduces oxidative damage, and protects membranes from stress-induced injury [26, 27].

Silicon alleviates salinity stress by enhancing photosynthetic efficiency, detoxifying reactive oxygen species (ROS), and regulating nutrient uptake [1]. For example, silicon application in 'Fuji' apple trees grafted onto M9 rootstocks under salt stress improved growth, stomatal conductance, chlorophyll content, and reduced electrolyte leakage [28]. Similarly, treating grapevine seedlings with 2 mM silicon under 100 mM NaCl stress improved growth, photosynthetic pigments, gas exchange, and soluble sugar accumulation [29]. Rootstocks are essential in modern fruit production, allowing fruit varieties to adapt to different environmental conditions [30]. Salt-tolerant rootstocks are especially valuable, as they reduce salinity damage and improve resource use efficiency [31]. GF677, a peach \times almond hybrid, is known for its vigorous growth, resistance to iron deficiency-induced chlorosis, and high productivity. Similarly, GN15, a cross between Spanish almond Grafi and Nemared peach, is characterized by strong growth, high yield potential, and tolerance to iron deficiency [32].

Momenpour et al. [33] found that almond genotypes grafted onto GF677 rootstock exhibited growth reductions, including decreases in scion and root fresh/dry weight, increased leaf necrosis, higher root-to-scion weight ratios, elevated ionic concentrations, and greater cell membrane damage as NaCl levels rose.

Salt stress negatively impacts growth and physiological functions in various cherry rootstocks [34]. For example, in CAB-6P cherry rootstock, NaCl-induced salinity reduced growth, impaired water relations, decreased chlorophyll content, and disrupted mineral balance [35]. In citrus rootstocks, including lemon, bitter orange, trifoliate orange, and Cleopatra mandarin, salinity stress resulted in reduced growth, lower relative water content, and imbalanced ion concentrations, with decreased K^+ and Ca^{2+} levels and increased Na^+ and Cl^- accumulation [36].

Silicon is well-known for enhancing photosynthesis under salt stress by reducing ion toxicity, minimizing ROS buildup, and protecting photosynthetic organelles [37, 38]. Studies on grapevines under salt stress showed that silicon increased free proline, total protein, and antioxidant enzyme activity while reducing hydrogen

peroxide levels [39]. In banana plants, silicon application stimulated shoot growth, decreased malondialdehyde and ion leakage, and improved photosynthetic efficiency and K^+ content, improving the K^+/Na^+ ratio [40].

In citrus rootstocks under salt stress, silicon improved growth, proline accumulation, antioxidant enzyme activity, and ion homeostasis by reducing Na^+ and Cl^- content, while enhancing peroxidase activity and proline levels [41]. A study on Fuji apple grafted onto MM 106 rootstock showed that silicon upregulated *SOS1* expression under both short- and long-term salt stress, while *NHX1* was upregulated only under short-term stress, indicating its role in sodium transport and stress adaptation in *Malus* species [42]. Similarly, in Myrobalan 29 C rootstock under drought conditions, silicon mitigated the adverse effects of stress by enhancing growth, relative leaf water content, and mineral uptake [43].

Despite these advances, the mechanisms through which silicon modulates ion transport genes and antioxidant systems in GF677 and GN15 rootstocks under salinity stress remain largely unexplored. Specifically, no studies have systematically evaluated the combined physiological and molecular responses of these two important rootstocks to silicon treatment and NaCl stress in controlled hydroponic conditions. Building on this gap, the present study hypothesizes that silicon enhances salinity tolerance in GF677 and GN15 rootstocks by improving growth, boosting antioxidant enzyme activity, and promoting osmolyte accumulation.

We expect silicon to mitigate NaCl-induced ion toxicity, oxidative stress, and water imbalance by modulating sodium transport genes and boosting stress adaptation. To test this, we will assess the response of GF677 and GN15 rootstocks to NaCl stress under controlled hydroponic and greenhouse conditions. We will measure physiological parameters such as root and shoot growth, ion leakage, MDA, H_2O_2 , RWC, antioxidant enzyme activity (catalase, guaiacol peroxidase, ascorbate peroxidase, superoxide dismutase), net photosynthesis, and osmolyte accumulation. Additionally, we will quantify Na^+ , Cl^- , K^+ , and Si concentrations and analyze the expression of sodium transport genes (*HKT1*, *SOS1*, *NHX1*, *AVP1*) via real-time PCR. Though conducted under controlled conditions, these findings may provide valuable insights for field applications and orchard management, ultimately improving salt tolerance in commercial fruit production.

Materials and methods

Plant materials and growth conditions

The experiment was conducted in the research greenhouse of the College of Agriculture, Urmia University, West Azerbaijan Province, Iran. A factorial design within a completely randomized block design (CRBD) was employed, incorporating three factors: silicon

concentrations, NaCl stress levels, and rootstocks, each with three replicates. The GF677 (*Prunus dulcis* × *Prunus persica*) and GN15 (*Prunus dulcis* × *Prunus persica*) rootstocks, obtained from Urum Zist Tak Company (Urmia, Iran), were propagated through shoot tip culture. Silicon, sourced from silicon dioxide (99.5% purity, Merck, Germany), was dissolved in distilled water to achieve final concentrations of 0, 1, and 2 mM. The concentrations used in this study were selected based on prior research on fruit trees [29, 39]. NaCl stress treatments included 0 mM (control), 50 mM, and 100 mM NaCl, which are commonly used in salinity studies to simulate moderate to severe stress levels [44, 45].

The electrical conductivity (EC) of the salt-treated solutions at 25 °C was 3.5 dS m⁻¹ for 50 mM NaCl and 7.9 dS m⁻¹ for 100 mM NaCl. To prevent salinity shock, NaCl was gradually introduced into the nutrient solutions at a rate of 50 mM per day until the target concentrations were reached. In September 2020, rootstocks approximately 15 cm in height were transplanted into plastic pots (16 cm diameter, 13 cm height) filled with a 1:1 perlite-to-peat moss mixture as part of a hydroponic system. The plants were grown under controlled greenhouse conditions with a 16-hour light/8-hour dark photoperiod, 40–60% relative humidity, and temperatures ranging from 17 °C to 27 °C. Fertigation was performed for six months using a modified half-strength Hoagland nutrient solution (pH 6.0), containing 2.5 mM $Ca(NO_3)_2$, 1 mM $MgSO_4$, 2.5 mM KNO_3 , 0.5 mM KH_2PO_4 , 0.3 μM $CuSO_4$, 6 μM $MnSO_4$, 0.7 μM $ZnSO_4$, 23 μM H_3BO_3 , 0.1 μM H_2MoO_4 , and 32 μM $FeSO_4$ [46]. The pH of the nutrient solution was adjusted to approximately 6 using 1 N hydrochloric acid (HCl), and the solution was freshly prepared every three days to ensure consistency and stability. The pH was monitored daily and adjusted as necessary.

Following a two-month acclimation period, the experiment commenced on April 7, 2021, and continued until June 8, 2021. Four experimental groups were established: (1) control (no silicon treatment) (2), NaCl stress without silicon (3), silicon treatments (1 mM and 2 mM), and (4) silicon treatments combined with NaCl stress. The treatments were applied for two months in the greenhouse. A total of 54 plants were used, with 27 pots per rootstock, each containing a single plant. The experiment was replicated three times. Silicon treatments (0, 1, and 2 mM) were applied every three days through the nutrient solution, while NaCl stress was gradually imposed to prevent salinity shock. Both treatments started simultaneously to ensure consistent exposure. Control plants received only the nutrient solution. The stress period lasted 60 days. On day 60, fully expanded young leaves from the middle section of the plants were collected for physiological and biochemical analyses. These included RWC, electrolyte

leakage, lipid peroxidation, hydrogen peroxide (H_2O_2), proline, total soluble sugars, glycine betaine, total soluble protein, antioxidant enzyme activity, mineral nutrient concentrations, and RNA extraction for gene expression analysis. Leaf samples were immediately frozen in liquid nitrogen and stored at -70°C for further analysis.

Fresh and dry weight of the shoots and roots

At the end of the experiment, the fresh weight of the shoots and roots was measured using a digital balance (PJ300, Mettler). To determine the dry weight, the samples were dried in an oven at 70°C for 72 h, and the dry weight was then recorded using the same digital balance.

Leaf relative water content (LRWC)

Leaf samples were collected from fully expanded leaves of all treatments, and their fresh weight was immediately recorded using a digital balance (PJ300, Mettler). The samples were then immersed in distilled water and stored in a refrigerator at 4°C for 24 h. After this period, the saturated weight of the leaves was measured. Subsequently, the leaves were dried at 70°C for 24 h, and their dry weight was recorded [47]. The relative water content of the leaves was calculated using the following formula:

$$RWC(\%) = (FW - DW) / (SW - DW) \times 100$$

FW = fresh weight, SW = saturated weight, DW = dry weight.

Electrolyte leakage (EL)

The method described by Lutts et al. [48] was used to measure ion leakage. Ten leaf discs (1 cm in diameter) were collected from fully expanded leaves. These samples were rinsed and placed in test tubes containing 10 mL of distilled water. The test tubes were kept at room temperature (25°C) for 4 h. The initial electrical conductivity (EC_1) was recorded using a conductivity meter (Cond./Temp./TDS/Salt/Logger 8306). The samples were then transferred to a water bath set at 100°C for 15 min. After cooling, the final electrical conductivity (EC_2) was measured. Electrolyte leakage was calculated using the following formula:

$$\text{Electrolyte leakage}(\%) = [EC_1/EC_2] \times 100$$

Hydrogen peroxide (H_2O_2)

To assess H_2O_2 content, 0.5 g of fresh leaf tissue was homogenized in a 0.1% trichloroacetic acid (TCA) solution and transferred to a 15 mL Falcon tube. The mixture was then centrifuged at 12000 rpm for 15 min. The reaction solution was prepared by combining 0.5 mL of 10 mM potassium phosphate buffer (pH 7), 1 mL of 1 M

potassium iodide (KI), and 0.5 mL of the plant extract. This mixture was incubated in the dark at 25°C for 1 h. Absorbance was measured at 390 nm using a spectrophotometer (Dynamico, HALO DB-20). Hydrogen peroxide concentration was calculated in micromoles per milligram of fresh weight, following the method of Velikova et al. [49].

Malondialdehyde (MDA)

To determine MDA levels, 0.2 g of frozen leaf tissue was homogenized in 5 mL of 1% trichloroacetic acid (TCA) solution. The resulting extract was then centrifuged at 8000 rpm for 10 min. One milliliter of the supernatant was mixed with 4 mL of a solution containing 20% TCA and 0.5% thiobarbituric acid (TBA). The mixture was incubated in a water bath at 95°C for 30 min, followed by rapid cooling in ice water. The samples were then centrifuged again at 8000 rpm for 5 min, and the supernatant was collected. Absorbance was measured at 532 and 600 nm using a spectrophotometer (Dynamico, HALO DB-20) [50]. MDA content was calculated using the extinction coefficient ($\text{mM}^{-1}\text{cm}^{-1} = 155$) and expressed as nanomoles per gram of fresh weight.

$$MDA (\text{nanomol g}^{-1}\text{FW}) = [A_{532} - A_{600}/155] \times 1000$$

Leaf net photosynthesis (Pn) and stomatal conductance

The net photosynthetic rate (Pn: $\mu\text{mol m}^{-2}\text{s}^{-1}$) and stomatal conductance for water vapor (gs: $\text{mol m}^{-2}\text{s}^{-1}$) were measured using a Photosynthesis Measurement System (Walz, HCM -1000, Germany) on clear, sunny days between 10:00 AM and 12:00 PM, following the methodology outlined by Haworth et al. [51]. During measurements, light intensity was maintained between 1200 and 1400 $\mu\text{mol photons m}^{-2}\text{s}^{-1}$, leaf temperature was kept at 20°C , CO_2 concentration was held at 350 ppm, and relative humidity ranged from 60 to 65%. Fully expanded leaves from the upper third of the main stem were used for all measurements.

Proline content measurement

Proline content was measured following the method of Irigoyen et al. [52]. A 0.5 g sample of fresh leaf tissue was ground in 5 mL of 95% ethanol and homogenized. The mixture was centrifuged at 3500 rpm for 10 min at 4°C . To the supernatant, 1 mL was added to 5 mL of ninhydrin reagent and 5 mL of glacial acetic acid in a test tube. The test tubes were placed in a 100°C water bath for 45 min. After cooling, 10 mL of benzene was added, and the mixture was shaken to transfer the proline into the benzene phase. The samples were allowed to stand for 30 min. Standard proline solutions with concentrations ranging from 0 to 0.1 $\mu\text{mol/mL}$ were prepared. The absorbance

of both the standard and sample solutions was measured at 515 nm using a spectrophotometer (Dynamico, HALO DB-20), and proline content was expressed as μmol per gram of fresh weight.

Total soluble sugars measurement

Total soluble sugars were measured using the method described by Irigoyen et al. [52]. For this, 0.5 g of fresh leaf tissue was ground in 5 mL of 95% ethanol and homogenized. The mixture was then centrifuged at 3500 rpm for 10 min at 4 °C. A 0.1 mL aliquot of the supernatant was combined with 3 mL of anthrone reagent in a test tube. The test tubes were placed in a warm water bath (bain-marie) for 10 min to allow the color to develop. After cooling, the absorbance of the samples was measured at 625 nm using a spectrophotometer (Dynamico, HALO DB-20). The total soluble sugar content was reported as milligrams per gram of fresh weight.

Glycine betaine content determination

The glycine betaine content was determined using the method described by Grieve and Grattan [53]. Initially, 0.25 g of dry leaf tissue was placed in a test tube with 10 mL of distilled water and shaken for 24 h. After filtering the solution through Whatman filter paper, 0.25 mL of the filtrate was combined with 0.25 mL of 2 N sulfuric acid in a test tube and placed in an ice bath for one hour. Next, 0.2 mL of potassium iodide (KI-I2) reagent was added, and the mixture was stored in the refrigerator at 4 °C for 16 h. Following this, the samples were centrifuged at 6000 rpm for 25 min, resulting in two phases. The upper phase was discarded, and the lower phase was treated with 6 mL of dichloroethane and vortexed several times. Finally, the absorbance of the resulting samples was measured at 365 nm using a spectrophotometer (Dynamico, HALO DB-20). The glycine betaine content in the leaf samples was calculated and reported as milligrams per gram of dry weight.

Total protein measurement

The Bradford method [54] was used to measure total protein content. Initially, 0.5 g of fresh leaf tissue was homogenized in a mortar with 5 mL of 50 mM sodium phosphate buffer on ice. The resulting homogenate was then centrifuged at 10,000 rpm for 20 min. A 100 μL aliquot of the clear supernatant was mixed with 2.5 mL of Coomassie Blue reagent. A standard solution was prepared using bovine serum albumin (BSA). The absorbance of both the samples and standards was measured at 595 nm using a spectrophotometer (Dynamico, HALO DB-20). The total protein content was expressed as micrograms per gram of fresh weight.

Preparation of plant extract for enzyme activity measurement

To prepare the plant extract and measure enzyme activities, 0.5 g of fresh leaf tissue was ground in a mortar with 3 mL of 50 mM Tris extraction buffer (pH=7.5). For ascorbate peroxidase activity, the extraction buffer was supplemented with 0.2 mM ascorbate. The homogenate was then centrifuged at 4,000 rpm for 20 min at 4 °C. The resulting supernatant was collected as the crude extract and used to determine the activities of catalase, peroxidase, and ascorbate peroxidase, following the method of Kang and Saltveit [55].

Catalase enzyme (CAT) activity measurement

Catalase activity was determined using the method of Aebi [56]. The reduction in absorbance at 240 nm was monitored over a 1-minute period using a spectrophotometer (Dynamico, HALO DB-20). The reaction mixture consisted of 2.5 mL of 50 mM phosphate buffer (pH 7), 0.2 mL of 1% hydrogen peroxide, and 0.3 mL of the plant extract. Catalase activity was expressed as units per milligram of protein.

Guaiacol peroxidase enzyme (GPX) activity

Guaiacol peroxidase activity was assessed by monitoring the increase in absorbance at 420 nm over a 1-minute period using a spectrophotometer (Dynamico, HALO DB-20) [57]. The reaction mixture consisted of 2.5 mL of 50 mM phosphate buffer (pH 7.5), 1 mL of 1% guaiacol, 0.1 mL of the plant extract, and 1 mL of 1% hydrogen peroxide. Guaiacol peroxidase activity was expressed as units per milligram of protein.

Ascorbate peroxidase enzyme (APX) activity

The activity of ascorbate peroxidase was measured by monitoring the decrease in absorbance at 290 nm, which reflects the oxidation of ascorbate, using a spectrophotometer (Dynamico, HALO DB-20) [58]. The reaction mixture consisted of 2.5 mL of 50 mM phosphate buffer (pH 7) with 0.1 mM EDTA and 1 mM sodium ascorbate, 0.2 mL of 1% hydrogen peroxide, and 0.1 mL of the plant extract. Ascorbate peroxidase activity was expressed as units per milligram of protein.

Superoxide dismutase enzyme (SOD) activity

Superoxide dismutase activity was assessed by measuring the inhibition of the photochemical reduction of NBT (nitroblue tetrazolium chloride), following the method outlined by Beauchamp and Fridovich [59]. The reaction mixture (3 mL) contained 50 mM phosphate buffer (pH=7.8), 13 mM methionine, 75 μM NBT, 0.1 mM EDTA, 2 μM riboflavin, and 0.1 mL of the enzyme extract (prepared for protein determination). The reaction was initiated at 25 °C and exposed to light for 10 min

using a 30-watt fluorescent lamp. Absorbance at 560 nm was measured using a spectrophotometer (Dynamico, HALO DB-20). The control sample included all components except the enzyme extract and light exposure. NBT undergoes photoreduction to form formazan, and one unit of superoxide dismutase activity is defined as the enzyme amount that inhibits 50% of the NBT photoreduction. The inhibition of NBT photoreduction, indicated by the absorbance difference between the samples and controls, was used to calculate enzyme activity, expressed as units per milligram of protein.

Mineral nutrients analysis

At the end of the experiment, mature leaves from the middle section of the stem and roots were collected and oven-dried at 70 °C for 48 h. The dried tissues (0.3–0.5 g) were finely ground and placed in porcelain crucibles. The samples were then ashed at 550 °C for 4–5 h to remove organic material, leaving behind white ash. The resulting ash was dissolved in 10 mL of 10 M hydrochloric acid to extract the inorganic components. Sodium (Na⁺) and potassium (K⁺) concentrations were determined using flame photometry (CORNING 400) following the method of Mizukoshi et al. [60]. Chloride (Cl⁻) concentration was measured by titration with 0.01 N silver nitrate (AgNO₃) solution, as described by Amami [61]. Silicon content was analyzed using an autoclave digestion and colorimetric method [62], with absorbance measured at 820 nm using a spectrophotometer. Results were expressed as a percentage of silicon.

RNA isolation and cDNA synthesis

Total RNA was extracted from plant tissues using the RNA Extraction Kit (Gene X, Tehran, Iran), following the manufacturer's protocol. Briefly, 80 mg of plant tissue (leaf or root) was ground in liquid nitrogen, and 800 µL of lysis buffer was added. The extraction process involved phase separation with chloroform, RNA precipitation, and purification using spin columns. The purified RNA was eluted in 100 µL of DEPC-treated water and stored at -80 °C. RNA integrity was assessed via 1.2% (w/v) agarose

gel electrophoresis, while RNA concentration and purity were determined using a NanoDrop spectrophotometer (NanoDrop ND-2000, Thermo Scientific, USA). The A260/A280 and A260/A230 absorbance ratios were measured to ensure RNA quality. To eliminate potential genomic DNA contamination, total RNA was treated with DNase I (Thermo Scientific, USA) according to the manufacturer's protocol.

The DNase treatment reaction consisted of 1 µL extracted RNA, 1 µL magnesium chloride reaction buffer, 1 µL DNase I, and DEPC-treated water, adjusted to a final volume of 10 µL. The reaction was incubated at 37 °C for 30 min, followed by enzyme inactivation with 1 µL of 50 mM EDTA at 65 °C for 10 min. To verify the absence of genomic DNA contamination, negative controls, including a no-reverse transcriptase (-RT) control and a no-template control (NTC), were included. For cDNA synthesis, 1 µg of total RNA was used as a template in a reaction prepared with the SMOBIO cDNA Synthesis Kit (Hsinchu, Taiwan), following the manufacturer's guidelines. The synthesized cDNA was stored at -20 °C for subsequent analysis.

Real-time PCR reactions

Relative gene expression was quantified using real-time PCR (ABI StepOne Plus, Applied Biosystems, Waltham, MA, USA). Gene-specific primers were designed based on conserved sequences within the Rosaceae family and synthesized by TAG Copenhagen. Primer validation was performed using Gene Runner software and BLAST searches in the NCBI GenBank database. PCR reactions were conducted in a total volume of 15 µL using AMPLIQON SYBR Green Master Mix, following the manufacturer's protocol. Each reaction contained 1 µL cDNA, 5.5 µL PCR-grade water, 7.5 µL 2X Master Mix, and 0.5 µL of each forward and reverse primer. The thermal cycling conditions included an initial enzyme activation at 95 °C for 15 min, followed by 40 amplification cycles consisting of denaturation at 95 °C for 15 s, annealing at an optimized temperature for 1 min, and fluorescence signal acquisition at 72 °C for 20 s (Table 1). The optimal

Table 1 Primer sequences used for real time PCR analysis in GF677 and GN15 rootstocks

Row	Primer Name	Primer Sequence	Length (bp)	Annealing Temperature (°C)
1	<i>HKT1-F</i>	F: 5'-TCACCTCTGTCTCTGCCTCAA-3'	21	58
	<i>HKT1-R</i>	R: 5'-AAGACCTCCCCACCTATGAACA-3'	22	
2	<i>AVP1-F</i>	F: 5'-ACCGAGTATCAGTATGTTGGGG-3'	22	58
	<i>AVP1-R</i>	R: 5'-GCAGGGTTGGCTCTTTGTG-3'	19	
3	<i>NHX1-F</i>	F: 5'-GAGGTGATCTGGGTAGCC-3'	18	58
	<i>NHX1-R</i>	R: 5'-ACACTGGACGCATGAAGG-3'	18	
4	<i>SOS1-F</i>	F: 5'-ATGGCGACGGTGACAGAATG-3'	20	58
	<i>SOS1-R</i>	R: 5'-CGAATGCCACTGCGTCCG-3'	18	
5	<i>EF1A-F</i>	F: 5'-CGAGAACATGATTACTGGAACCTC-3'	24	58
	<i>EF1A-R</i>	R: 5'-CATCCATCTTGTTACAGCAGCA-3'	22	

annealing temperature was determined using melting curve analysis and agarose gel electrophoresis to confirm amplicon specificity. The EF1A gene was used as an internal reference, and relative gene expression levels were calculated using the $2^{-\Delta\Delta C_t}$ method [63]:

$$\Delta C_t = C_t (\text{Target}) - C_t (\text{Reference}).$$

Statistical analysis

The experiment followed a factorial design within a completely randomized block design (CRBD) with three replicates. It examined the effects of three silicon concentrations, three NaCl stress levels, and two rootstocks, resulting in 18 treatment combinations and a total of 54 experimental units. Data were analyzed using analysis of variance (ANOVA) in SAS 9.4 (SAS Institute, Cary, NC, USA), and treatment means were compared using Duncan's multiple range test ($p \leq 0.05$).

Results

Plant growth parameters

Fresh, and dry weight of shoots

The physiological, biochemical, and molecular responses of GF677 and GN15 rootstocks were assessed under control, salinity stress, silicon supplementation, and combined NaCl+silicon treatments. Figure 1A illustrates that increasing NaCl concentrations significantly reduced shoot fresh weight in both rootstocks, demonstrating a clear inhibitory effect of salinity on aboveground biomass production. Under non-saline conditions (0 mM NaCl), GF677 exhibited a higher shoot fresh weight than GN15, reflecting its inherently more vigorous shoot growth capacity. As NaCl levels rose to 50 and 100 mM, both rootstocks experienced a progressive decline in shoot biomass; however, the reduction was more pronounced in GN15, indicating a higher sensitivity to salt-induced growth inhibition.

A comparable trend was observed for shoot dry weight (Fig. 1B), which decreased with increasing NaCl in both genotypes. Under control conditions, GF677 accumulated significantly more dry shoot biomass than GN15, reinforcing its stronger baseline performance. At 50 mM NaCl, both rootstocks experienced notable reductions, yet GN15 again suffered greater losses, suggesting its limited capacity to cope with even moderate salt stress. At 100 mM NaCl, shoot dry weight declined to its lowest point, particularly in GN15, underscoring the cumulative impact of high salinity on shoot tissue development.

Figure 1C further reveals that silicon application mitigated these salinity-induced losses in shoot fresh weight. While no significant differences were observed under non-saline conditions, 2 mM silicon application under both 50 and 100 mM NaCl significantly improved shoot fresh weight compared to untreated plants, indicating that the beneficial effects of silicon become evident

primarily under stress. Notably, plants grown under saline conditions without silicon exhibited the lowest shoot fresh weights, highlighting silicon's critical role in protecting shoot growth under adverse environmental conditions.

A similar pattern was observed in shoot dry weight responses (Fig. 1D). Silicon application had minimal effect under non-stress conditions, but under NaCl stress, particularly at 100 mM NaCl, 2 mM silicon significantly enhanced shoot dry biomass. These results collectively point to the stress-specific efficacy of silicon, suggesting that it alleviates salinity-induced growth suppression—potentially through improved water retention, ion regulation, and modulation of physiological stress responses that maintain shoot function and integrity under salt stress.

Fresh and dry weight of roots

Across all NaCl concentrations, GF677 consistently exhibited higher root fresh weight than GN15, suggesting a stronger capacity to sustain root growth under saline conditions. Although NaCl significantly reduced root fresh weight in both rootstocks, the most pronounced decline was observed at 100 mM NaCl (Fig. 1E), indicating that elevated salinity levels strongly inhibit root development in both genotypes. Nonetheless, the less drastic reduction in GF677 points to its greater resilience compared to GN15.

Similarly, root dry weight declined progressively with increasing NaCl in both rootstocks. However, GF677 consistently maintained higher values, reflecting a better ability to preserve root biomass under stress (Fig. 1F). At 50 mM NaCl, GF677 and GN15 were categorized into groups "b" and "d," respectively, showing that moderate salinity already compromises root development, particularly in GN15. Under severe salinity (100 mM NaCl), this effect was further amplified, with GF677 assigned to group "c" and GN15 to group "e," which recorded the lowest root dry weight values. These results reinforce the notion that GF677 possesses a relatively higher salt tolerance than GN15, possibly due to more efficient stress mitigation mechanisms.

Under non-saline conditions, root fresh weight remained high across all silicon treatments, with no significant differences observed (Fig. 1G), indicating that silicon has little to no effect on root growth when plants are not exposed to stress. However, at 50 mM NaCl, salinity-induced reductions in root fresh weight became evident. Notably, silicon supplementation—particularly at 2 mM—substantially alleviated these reductions, resulting in significantly higher root fresh weight compared to the non-silicon control. This improvement suggests that silicon enhances salt tolerance by supporting root development under moderate salinity, likely through mechanisms

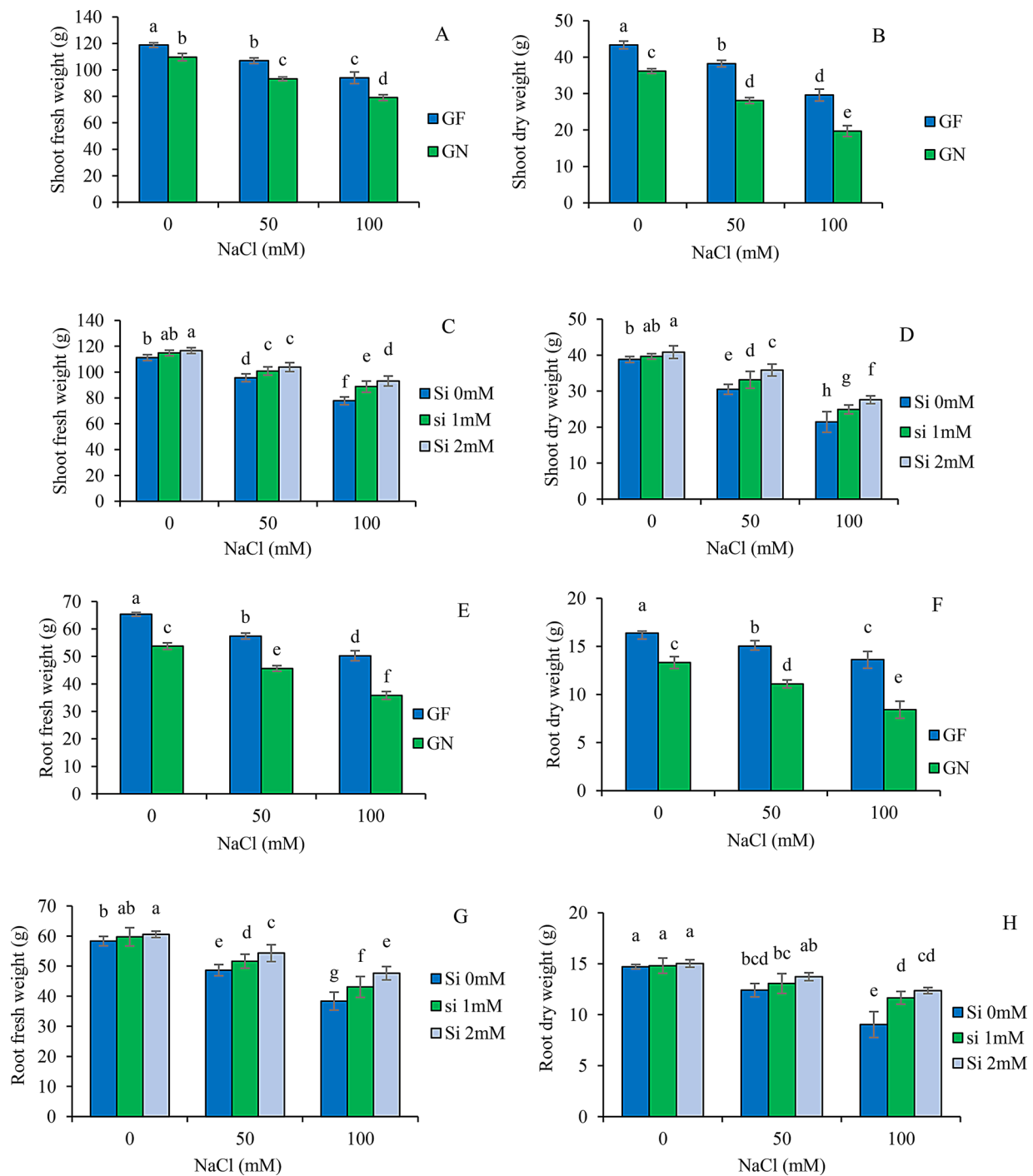


Fig. 1 Effects of NaCl (0, 50, and 100 mM) and silicon (0, 1, and 2 mM) treatments on shoot fresh weight (A, C), shoot dry weight (B, D), root fresh weight (E, G), and root dry weight (F, H) in two rootstocks, GF677 and GN15. Different letters indicate statistically significant differences according to Duncan's multiple range test ($p < 0.05$)

such as improved water retention or reduced oxidative stress. Under severe salinity (100 mM NaCl), root fresh weight declined further in all treatments, reflecting the intensified impact of high salt levels on plant vitality. Yet, the 2 mM silicon treatment again showed the strongest protective effect, underscoring its potential in enhancing

root system resilience even under harsh saline conditions. These findings collectively highlight the beneficial role of silicon in mitigating salt-induced root growth inhibition, with the effect becoming more pronounced as the severity of stress increases.

Figure 1H shows that under non-saline conditions, root dry weight remained relatively stable across all silicon treatments, emphasizing that silicon has no notable impact on root biomass when plants are not subjected to stress. However, at 50 mM NaCl, salinity led to a reduction in root dry weight. Interestingly, the application of 2 mM silicon significantly mitigated this loss, suggesting that silicon contributes to the maintenance of root dry biomass under moderate salt stress, possibly by enhancing root structure integrity or osmotic adjustment. Under severe salinity stress (100 mM NaCl), the decline in root dry weight became more pronounced, with the lowest values observed in the absence of silicon. Conversely, plants treated with 2 mM silicon retained significantly more root biomass, indicating a strong protective effect. These results reinforce the view that silicon supplementation, particularly at optimal concentrations, enhances root tolerance to salinity by preserving structural biomass even under intense stress conditions.

Relative water content, electrolyte leakage, malondialdehyde, and hydrogen peroxide content

At 50 and 100 mM NaCl, relative water content (RWC) declined significantly in both rootstocks, indicating that salinity impairs the plant's ability to retain water by disrupting osmotic balance and water uptake. However, the application of silicon (1 and 2 mM) effectively mitigated this reduction, suggesting a protective role in maintaining cellular hydration under salt stress conditions. Notably, the highest RWC at 100 mM NaCl was observed with 2 mM silicon, highlighting its superior efficacy in enhancing water retention and alleviating osmotic stress in saline environments (Fig. 2A).

Electrolyte leakage (EL), a widely recognized indicator of membrane integrity, increased significantly under 100 mM NaCl, with GN15 exhibiting the highest ion leakage (30.62%), implying that its cell membranes are more susceptible to salt-induced oxidative damage. This response underscores GN15's heightened vulnerability to salinity. In contrast, silicon treatment markedly reduced ion leakage at both 1 and 2 mM concentrations, demonstrating its membrane-stabilizing effect under stress. At 100 mM NaCl, 1 mM and 2 mM silicon applications reduced electrolyte leakage by 13.57% and 24.01%, respectively, compared to non-supplemented plants, indicating that silicon not only limits membrane damage but may also enhance antioxidant or structural defense mechanisms under salinity stress (Fig. 2B, C).

Malondialdehyde (MDA) levels, a biomarker of lipid peroxidation and oxidative damage, increased significantly under 100 mM NaCl, particularly in the absence of silicon. Compared to the control, MDA levels rose by 74% in GF677 and 86% in GN15, indicating that salinity triggers substantial oxidative stress, with GN15 exhibiting

greater membrane damage than GF677. However, silicon application markedly reduced MDA accumulation across all treatments, with 2 mM Si exerting a stronger effect than 1 mM. This suggests that silicon mitigates salt-induced oxidative damage, likely by enhancing antioxidant defense mechanisms or stabilizing cellular membranes (Fig. 2D). Similarly, salinity stress led to a notable accumulation of hydrogen peroxide (H_2O_2), a reactive oxygen species associated with oxidative stress signaling and damage. At 100 mM NaCl, H_2O_2 levels increased twofold in GF677 and 2.5-fold in GN15 compared to control conditions, reflecting the heightened oxidative burden induced by severe salinity, especially in GN15. Silicon supplementation effectively lowered H_2O_2 levels under both control and salt stress, with 2 mM Si again proving more effective. These results indicate that silicon alleviates oxidative stress by reducing reactive oxygen species accumulation, thereby contributing to cellular homeostasis under salinity (Fig. 2E).

Compatible osmolytes (Proline, total soluble sugars, Glycine Betaine, and total soluble Protein)

Proline and total soluble sugars

Salinity stress markedly increased proline accumulation in the leaves of both rootstocks, with GN15 exhibiting a stronger response than GF677. Under 100 mM NaCl, proline content in GN15 reached 1.9 times the control level, indicating a more pronounced osmotic adjustment strategy in this genotype. Interestingly, silicon supplementation under salt stress significantly reduced proline levels in both rootstocks, particularly at higher concentrations, suggesting that silicon alleviates osmotic stress, thereby diminishing the plant's reliance on proline accumulation for cellular water balance (Fig. 3A, B).

A similar pattern was observed for soluble sugars. Under non-stress conditions, silicon had little effect on sugar accumulation. However, under salinity, NaCl significantly increased soluble sugar content in both genotypes, especially in GN15, indicating its greater dependence on sugar-mediated osmoprotection. Silicon treatment effectively reduced soluble sugar levels under salt stress, with the most pronounced decrease observed at 2 mM Si. This implies that silicon may mitigate the osmotic burden imposed by salinity, reducing the need for excessive sugar accumulation as a stress response. The lowest sugar levels were recorded in GF677 under control conditions, while the highest appeared in GN15 exposed to 100 mM NaCl without silicon, highlighting the differential osmotic responses between the genotypes and the modulatory effect of silicon (Fig. 3C).

Glycine-betaine and total soluble protein

Glycine betaine levels increased in both rootstocks in response to NaCl stress, with the highest accumulation

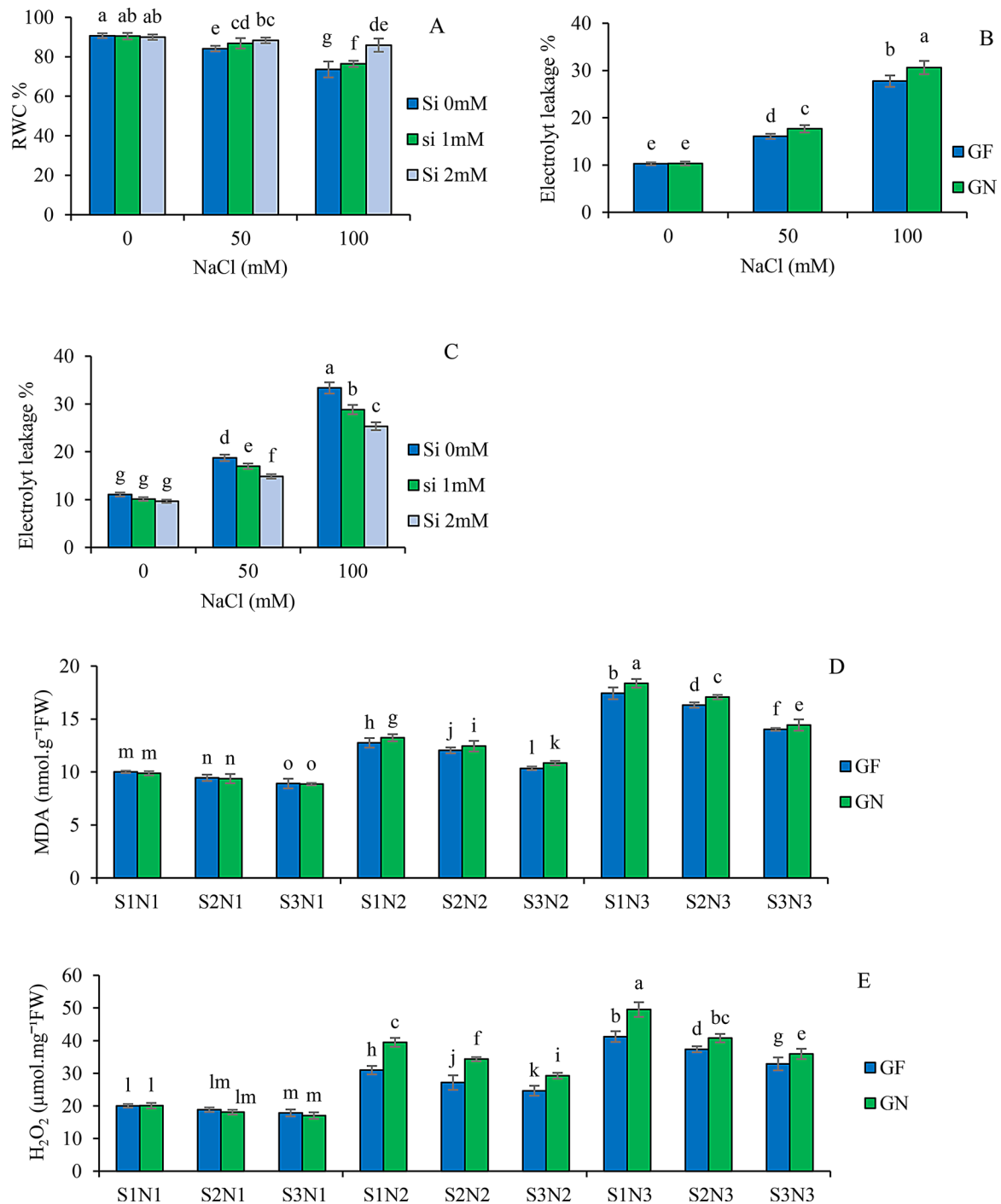


Fig. 2 Effects of NaCl (0, 50, and 100 mM) and silicon (0, 1, and 2 mM) treatments on relative water content (RWC; **A**), electrolyte leakage (**B**, **C**), malondialdehyde (MDA; **D**), and hydrogen peroxide (H₂O₂; **E**) in leaves of two rootstocks, GF677 and GN15. Treatment codes: N1=0 mM NaCl, N2=50 mM NaCl, N3=100 mM NaCl; S1=0 mM Si, S2=1 mM Si, S3=2 mM Si. Different letters indicate statistically significant differences according to Duncan's multiple range test ($p < 0.05$)

observed at 100 mM NaCl—3.3-fold higher than the control in GF677 and 2.8-fold in GN15—indicating its role as a compatible solute aiding in osmotic adjustment under salinity. Notably, silicon application further enhanced glycine betaine levels under both control and stress

conditions, particularly at 2 mM, suggesting that silicon may promote osmoprotectant accumulation as part of its stress mitigation strategy (Fig. 3D).

As shown in Fig. 3E, total protein content increased significantly under moderate salinity (50 mM NaCl),

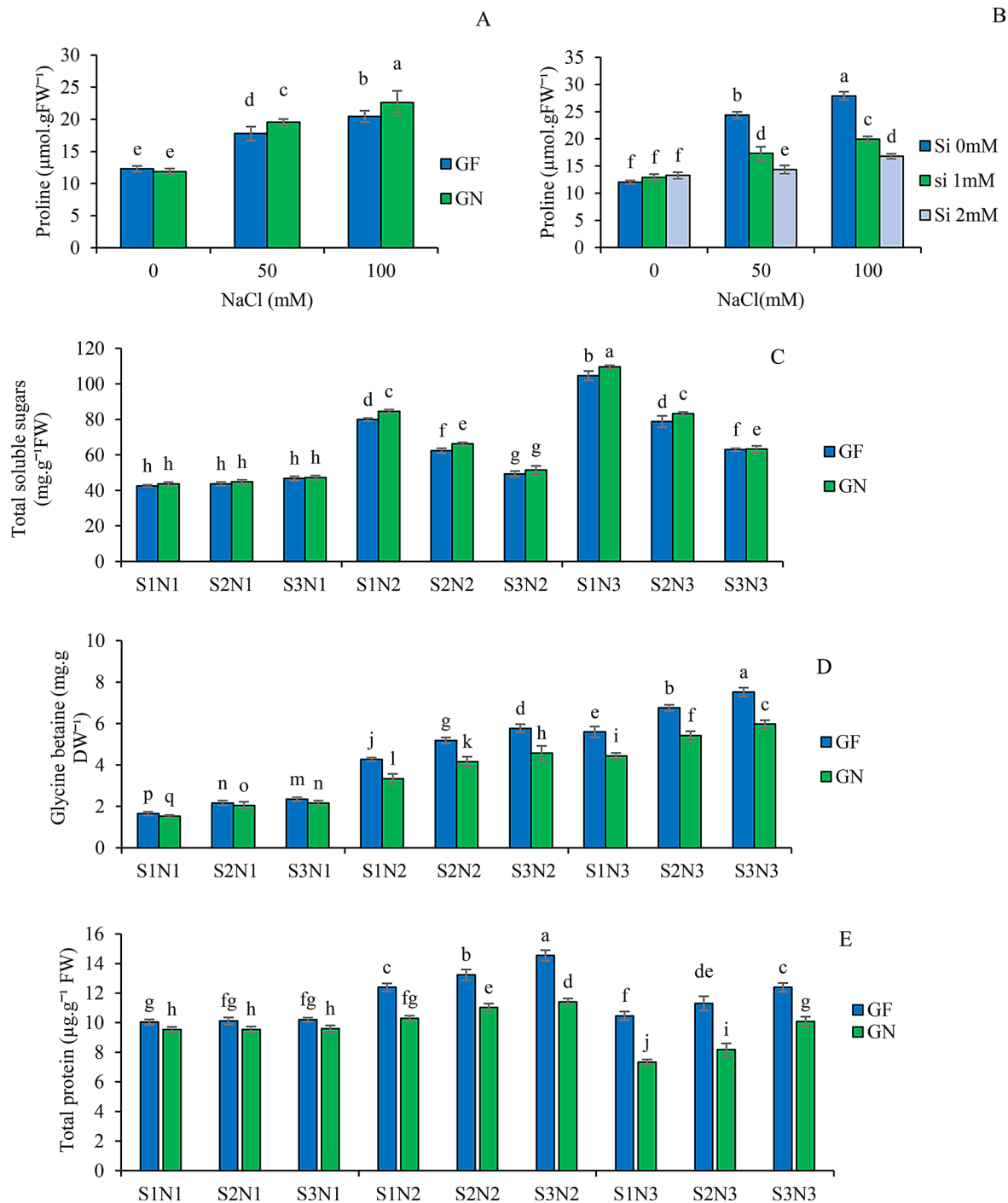


Fig. 3 Effects of NaCl (0, 50, and 100 mM) and silicon (0, 1, and 2 mM) treatments on proline content (A, B), total soluble sugars (C), glycine betaine (D), and total protein (E) in leaves of two rootstocks, GF677 and GN15. Treatment codes: N1 = 0 mM NaCl, N2 = 50 mM NaCl, N3 = 100 mM NaCl; S1 = 0 mM Si, S2 = 1 mM Si, S3 = 2 mM Si. Different letters indicate statistically significant differences according to Duncan's multiple range test ($p < 0.05$)

especially in GF677, with the highest level recorded in plants treated with 2 mM silicon (S_3N_2). This pattern suggests that under moderate stress, silicon may either enhance protein synthesis or protect functional proteins against degradation. However, severe salt stress (100 mM NaCl) led to a marked decline in total protein

levels, particularly in GN15, reflecting increased protein degradation or impaired synthesis under high stress conditions. Silicon supplementation, especially at 2 mM, alleviated this reduction and maintained higher protein levels, particularly in GF677, highlighting silicon's

protective role in preserving protein integrity and supporting cellular function under severe salinity.

Antioxidant enzymes (Catalase, Guaiacol peroxidase, ascorbate peroxidase, superoxide Dismutase)

Catalase (CAT) activity significantly increased in response to 100 mM NaCl, rising by 2.14-fold in GF677 and 1.88-fold in GN15 compared to the control, indicating an enhanced oxidative stress response in both rootstocks under high salinity. Silicon application further amplified CAT activity under salt stress, with the 2 mM treatment producing the strongest effect, suggesting that silicon reinforces the antioxidant defense system by stimulating catalase activity (Fig. 4A).

Guaiacol peroxidase (GPX) activity followed a similar trend, increasing markedly under salinity, with the highest activity observed at 100 mM NaCl. At this level, activity increased 2.3-fold in GF677 and 2-fold in GN15, reflecting the induction of peroxidase-mediated scavenging of hydrogen peroxide as a protective mechanism. The application of silicon further enhanced GPX activity, particularly at 2 mM, highlighting silicon's role in strengthening antioxidative capacity under salt stress (Fig. 4B, C).

Ascorbate peroxidase (APX) activity also rose under increasing salinity, peaking at 100 mM NaCl, which indicates an intensified enzymatic effort to neutralize ROS during severe stress. Silicon supplementation, especially at 2 mM, significantly elevated APX activity beyond levels seen under salinity alone, supporting the notion that silicon helps optimize enzymatic ROS detoxification pathways (Fig. 4D, E).

Superoxide dismutase (SOD) activity increased by 56.96% in GF677 and 51.84% in GN15 at 100 mM NaCl compared to the control, demonstrating the activation of primary defense mechanisms against superoxide radicals under salt stress. The addition of silicon further boosted SOD activity, particularly at 2 mM, implying that silicon modulates the antioxidative machinery by enhancing ROS detoxification through SOD activity (Fig. 4F, G).

Net photosynthesis and stomatal conductance

As NaCl stress intensified, net photosynthesis (Pn) declined significantly in both rootstocks, with GN15 exhibiting a sharper reduction than GF677, indicating greater photosynthetic sensitivity to salinity in GN15. At 50 mM NaCl, salinity moderately reduced Pn, but silicon application—especially at 2 mM—alleviated this decline, suggesting that silicon helps maintain photosynthetic function under moderate stress. At 100 mM NaCl, Pn decreased dramatically in both genotypes; however, 2 mM Si treatment significantly mitigated the adverse effects, preserving higher photosynthetic rates relative to untreated plants. These findings suggest that while salinity exerts a strong inhibitory effect on photosynthesis,

silicon supplementation—particularly at 2 mM—supports photosynthetic resilience, with the most notable benefits observed under moderate and severe stress conditions (Fig. 5A, B).

Stomatal conductance (gs) followed a similar trend. The highest gs values were recorded in control plants, especially in GN15, indicating superior baseline stomatal performance. Increasing NaCl concentrations progressively reduced gs in both rootstocks, with GN15 again showing a greater decline, highlighting its vulnerability to salinity-induced stomatal closure. Under non-saline conditions, silicon had no significant impact on gs, indicating minimal influence under optimal conditions. However, at 50 mM NaCl, silicon—particularly at 2 mM—attenuated the reduction in gs, suggesting that silicon helps sustain stomatal function under moderate salt stress. At 100 mM NaCl, gs declined further, yet 2 mM Si-treated plants maintained significantly higher conductance than their non-silicon counterparts, demonstrating silicon's role in partially restoring gas exchange under severe salinity (Fig. 5C, D).

Effects of NaCl on mineral nutrients

Na⁺ and Cl⁻ concentration in leaf and root

Increasing NaCl concentration from 0 to 50 and 100 mM resulted in a significant increase in root Na⁺ content, with the highest accumulation observed at 100 mM NaCl. Silicon application (1 and 2 mM) effectively reduced Na⁺ uptake in roots, particularly under high salinity. At 100 mM NaCl, the control plants exhibited the highest Na⁺ accumulation, while the 2 mM Si treatment led to the lowest levels, suggesting that silicon may help limit sodium uptake and accumulation under severe salt stress. Similarly, NaCl stress caused a marked increase in Na⁺ accumulation in leaves, with the highest levels at 100 mM NaCl. Silicon supplementation, particularly at 2 mM, effectively reduced leaf Na⁺ uptake, indicating that silicon plays a key role in limiting the translocation of Na⁺ into aboveground tissues. Across both rootstocks, Na⁺ accumulation was more pronounced in GN15 than in GF677, further confirming the greater salt sensitivity of GN15 (Fig. 6A–D).

At 0 mM NaCl, Cl⁻ accumulation was low across all silicon treatments, with no significant differences observed. Under 50 mM NaCl, leaf Cl⁻ content significantly increased, although silicon had no noticeable effect on Cl⁻ uptake. However, under 100 mM NaCl, Cl⁻ levels peaked, with the highest accumulation occurring in the control plants. Silicon application, particularly at 2 mM, significantly decreased Cl⁻ accumulation, highlighting its protective role in mitigating excessive chloride uptake under severe salinity stress. In roots, Cl⁻ accumulation was minimal at 0 mM NaCl and remained unaffected by silicon treatments. At 50 mM NaCl, Cl⁻ content increased

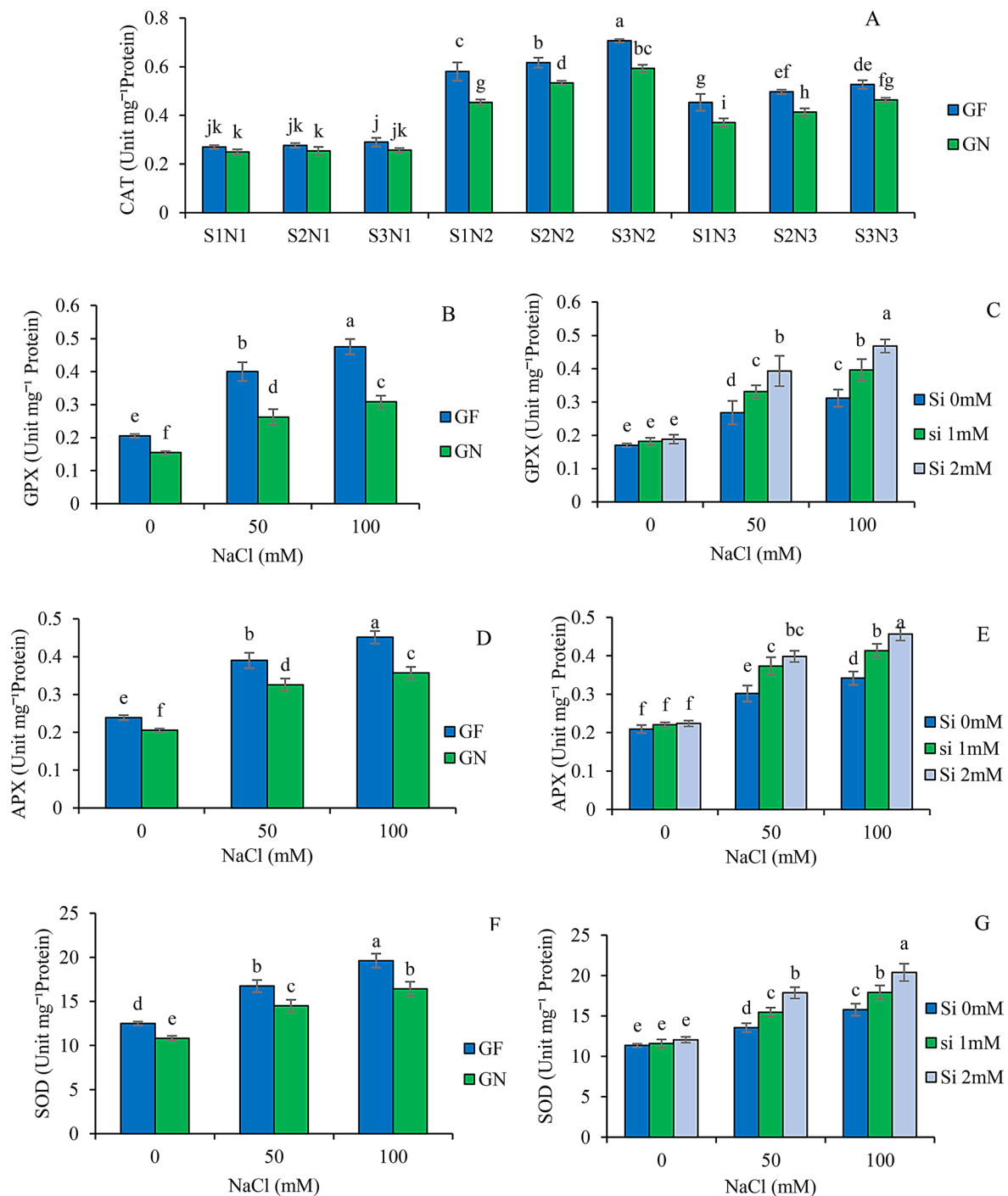


Fig. 4 Effects of NaCl (0, 50, and 100 mM) and silicon (0, 1, and 2 mM) treatments on the activities of catalase (CAT; **A**), guaiacol peroxidase (GPX; **B, C**), ascorbate peroxidase (APX; **D, E**), and superoxide dismutase (SOD; **F, G**) in leaves of two rootstocks, GF677 and GN15. Treatment codes: N1 = 0 mM NaCl, N2 = 50 mM NaCl, N3 = 100 mM NaCl; S1 = 0 mM Si, S2 = 1 mM Si, S3 = 2 mM Si. Different letters indicate statistically significant differences according to Duncan's multiple range test ($p < 0.05$)

significantly, but again, silicon had no effect. However, at 100 mM NaCl, 2 mM Si significantly reduced Cl^- accumulation in roots, suggesting that silicon may help minimize chloride-induced toxicity. In contrast, the 1 mM Si treatment had a slight, non-significant effect on

Cl^- levels. These results suggest that silicon, especially at 2 mM, plays a significant role in limiting both Na^+ and Cl^- accumulation under high salinity, thereby reducing the potential for salt stress-induced damage (Fig. 6E, F).

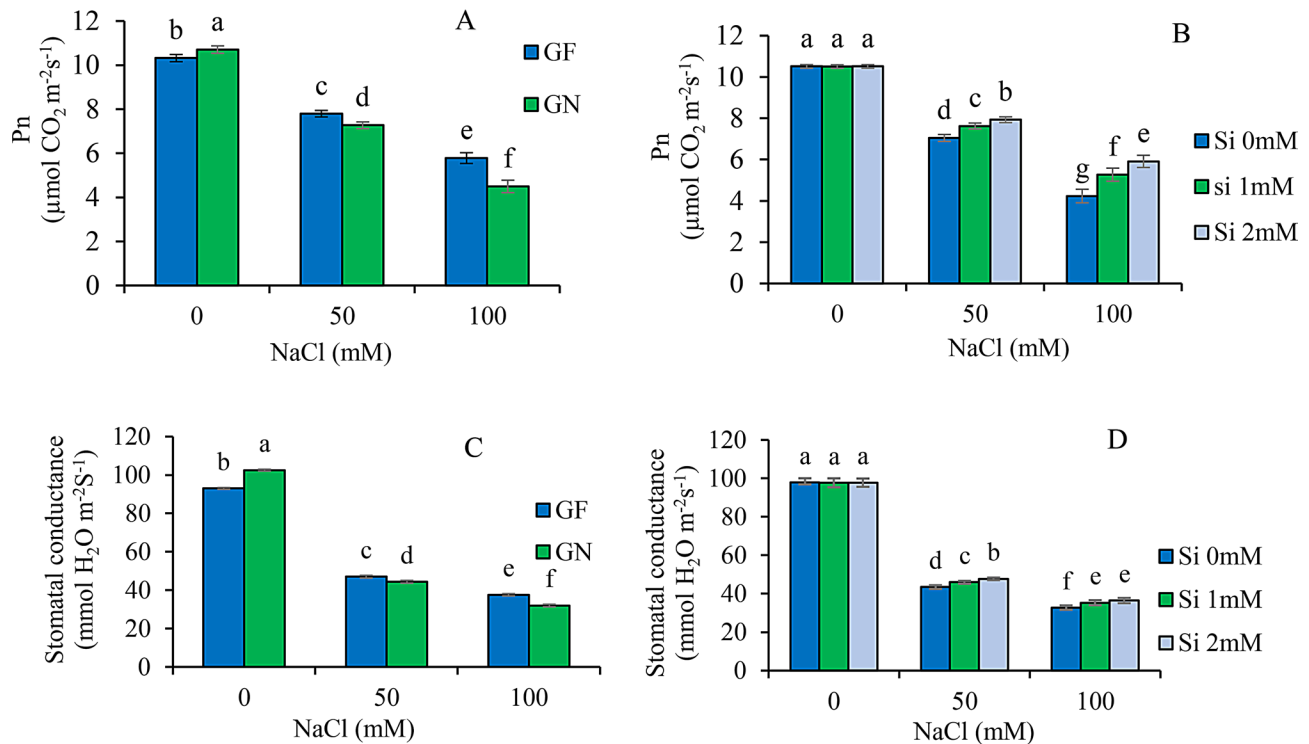


Fig. 5 Effects of NaCl (0, 50, and 100 mM) and silicon (0, 1, and 2 mM) treatments on net photosynthetic rate (Pn; **A, B**) and stomatal conductance (**C, D**) in leaves of two rootstocks, GF677 and GN15. Treatment codes: N1 = 0 mM NaCl, N2 = 50 mM NaCl, N3 = 100 mM NaCl; S1 = 0 mM Si, S2 = 1 mM Si, S3 = 2 mM Si. Different letters indicate statistically significant differences according to Duncan's multiple range test ($p < 0.05$)

***K⁺* and Si concentration in leaf and root**

Under non-saline conditions (0 mM NaCl), root K^+ levels remained stable across all silicon treatments. However, at 50 mM NaCl, root K^+ content declined significantly, with 2 mM Si providing a slight yet notable improvement in maintaining potassium levels. At 100 mM NaCl, root K^+ levels reached their lowest point, but 2 mM Si significantly reduced K^+ loss, while 1 mM Si offered moderate protection. These findings indicate that salinity-induced reductions in root K^+ content are likely due to Na^+ competition for uptake, and that silicon—especially at 2 mM—plays a crucial role in maintaining K^+ levels and ensuring ionic balance under salt stress.

Similarly, increasing NaCl concentrations from 0 to 50 and 100 mM significantly reduced leaf K^+ content, with the lowest values observed at 100 mM NaCl. Silicon supplementation (1 mM and 2 mM) effectively mitigated this decline, as both treatments helped maintain higher leaf K^+ levels compared to the untreated control (0 mM Si) across all salinity levels. Notably, at 100 mM NaCl, 2 mM Si resulted in the highest leaf K^+ content, while the control exhibited the lowest, further emphasizing the protective role of silicon in preserving potassium levels under high salinity stress (Fig. 6G–J).

Additionally, the mean comparison results revealed that NaCl stress reduced Si accumulation in both leaves and roots of both rootstocks. However, silicon

application increased Si content, especially in the roots, suggesting that silicon enhances its own uptake and accumulation under saline conditions (Fig. 6K–N).

Gene expression levels

NaCl stress induced an increase in *HKT1* gene expression in the leaves and roots of GF677 and in the roots of GN15 compared to the control. However, in the leaves of GN15, NaCl treatment alone did not result in a significant change in expression. The increase in *HKT1* expression was more pronounced in the roots than in the leaves for both rootstocks, suggesting that the roots play a central role in sodium uptake and transport under salinity stress. Silicon application, combined with NaCl stress, further enhanced *HKT1* expression in both organs. The highest expression level was observed in GF677 under NaCl combined with silicon, with a 1.66-fold increase in the leaves and a 4.72-fold increase in the roots compared to the control, indicating that silicon may augment the plant's ability to cope with salt stress by modulating ion transport (Fig. 7A, B).

Similarly, *AVP1* gene expression was upregulated by NaCl stress in both leaves and roots. Under NaCl treatment alone, relative expression increased 2.51-fold in the leaves and 3.07-fold in the roots of GF677, while in GN15, it rose 1.91-fold in the leaves and 1.54-fold in the roots compared to the control. Silicon application further

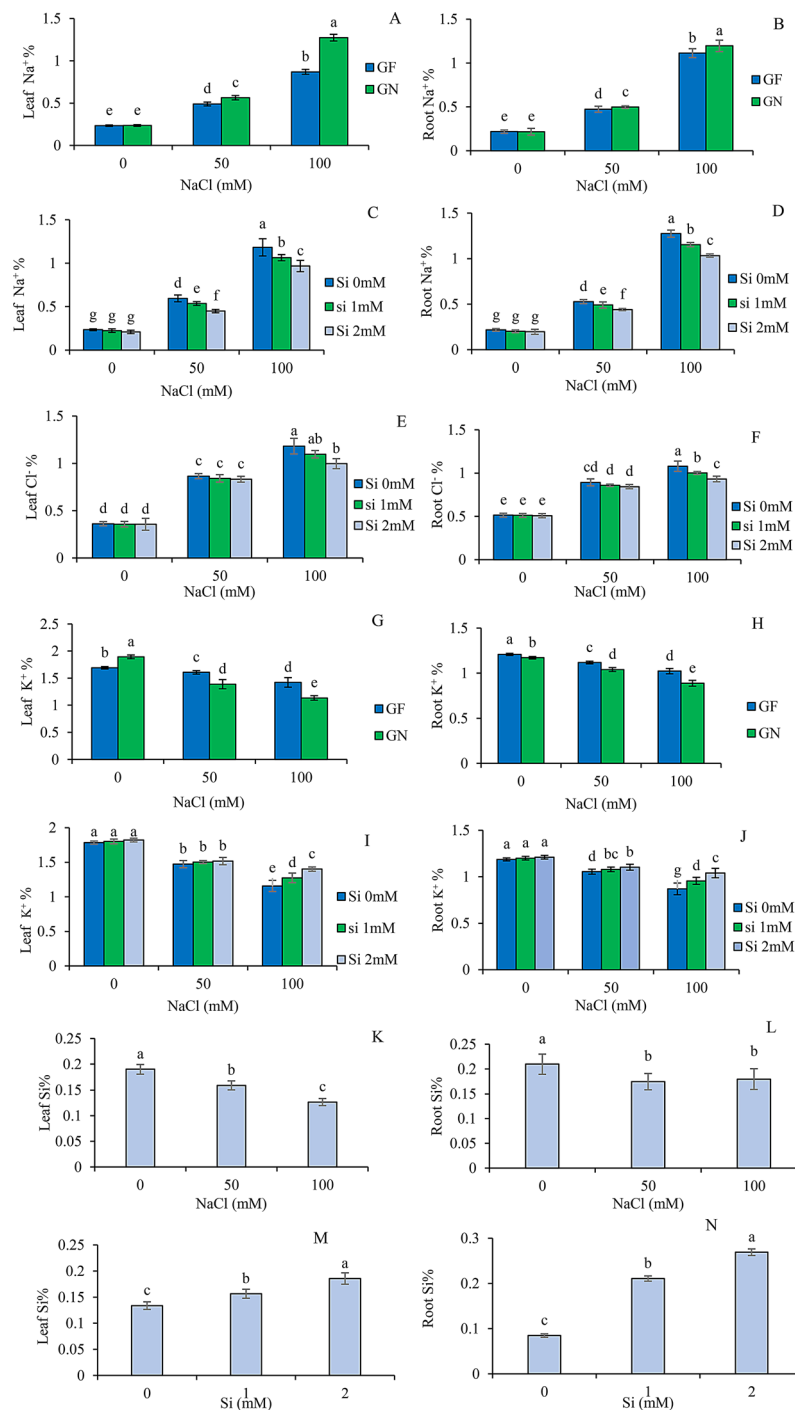


Fig. 6 Effects of NaCl (0, 50, and 100 mM) and silicon (0, 1, and 2 mM) treatments on Na⁺ content in leaves (A, C) and roots (B, D), Cl⁻ content in leaves (E) and roots (F), K⁺ content in leaves (G, I) and roots (H, J), and Si content in leaves (K, M) and roots (L, N) of two rootstocks, GF677 and GN15. Different letters indicate statistically significant differences according to Duncan's multiple range test ($p < 0.05$)

boosted *AVP1* expression, though in GN15 leaves, this increase was not significantly different from NaCl treatment alone. The highest *AVP1* expression was observed in GF677 under NaCl combined with silicon treatment, suggesting that silicon enhances the expression of genes

involved in vacuolar Na⁺ compartmentalization, contributing to improved salt tolerance (Fig. 7C, D).

Likewise, *NHX1* gene expression increased in both leaves and roots under NaCl stress. In the leaves, GF677 exhibited higher *NHX1* expression than GN15, while in the roots, no significant difference was observed between

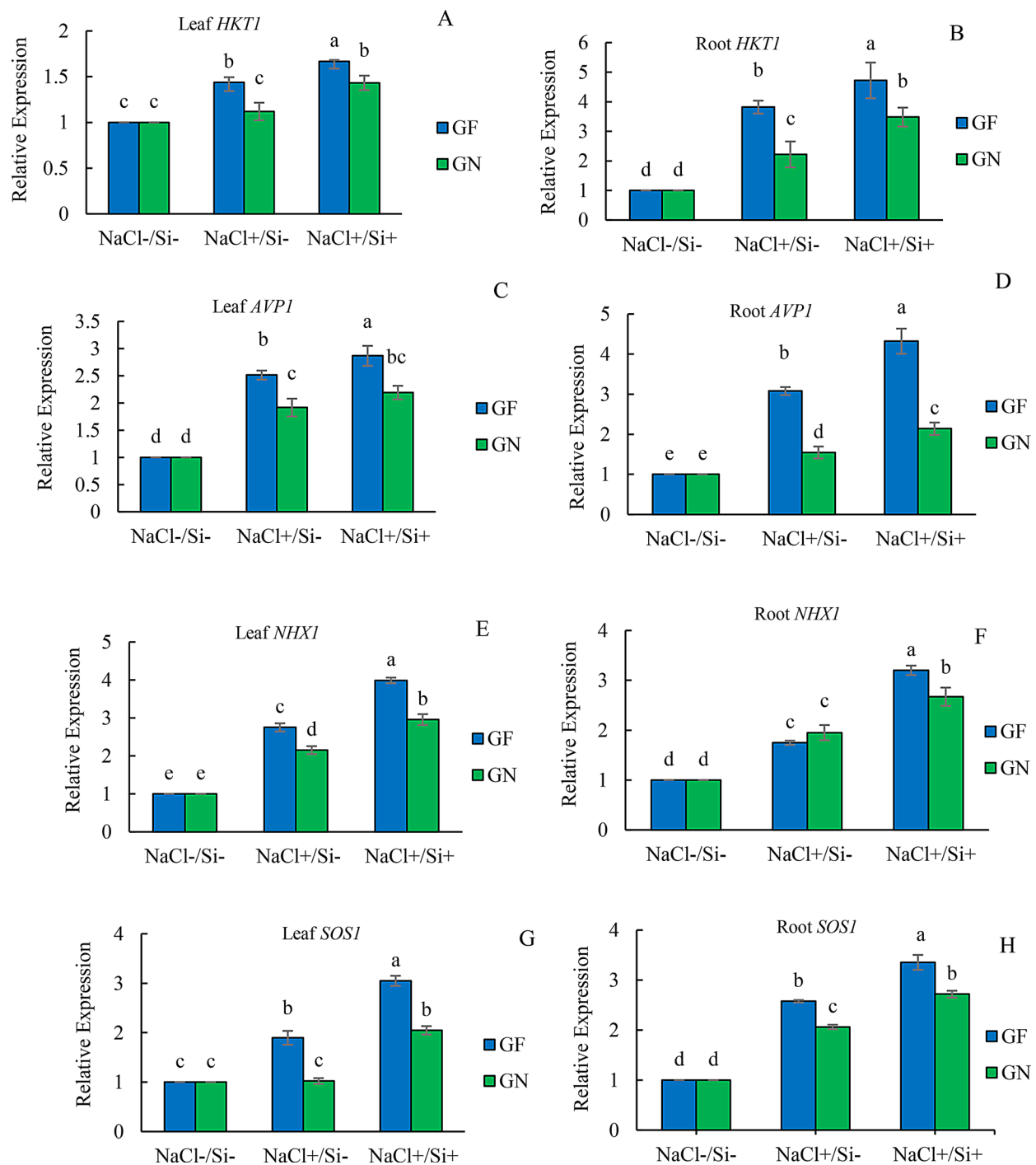


Fig. 7 Effects of NaCl (0, 50, and 100 mM) and silicon (0, 1, and 2 mM) treatments on the relative expression levels of *HKT1*, *AVP1*, *NHX1*, and *SOS1* genes in leaves (A, C, E, G) and roots (B, D, F, H) of two rootstocks, GF677 and GN15. Different letters indicate statistically significant differences according to Duncan's multiple range test ($p < 0.05$)

the two rootstocks. Silicon treatment further upregulated *NHX1* expression in both leaves and roots, with the highest levels recorded in GF677 under NaCl combined with silicon treatment. This suggests that silicon may promote the activity of sodium/proton antiporters, such as *NHX1*,

which are involved in maintaining cellular ion homeostasis during salt stress (Fig. 7E, F).

NaCl stress also enhanced the expression of *SOS1* in both leaves and roots. Compared to the control, *SOS1* expression in GF677 increased 1.89-fold in the leaves and 2.57-fold in the roots, while in GN15, it increased

1.22-fold in the leaves and 2.06-fold in the roots. Overall, *SOS1* expression was higher in the roots than in the leaves for both rootstocks. Silicon application further upregulated *SOS1* expression, with the highest levels observed in GF677 under NaCl combined with silicon treatment, indicating that silicon may help enhance the function of the *SOS* pathway, which is crucial for maintaining sodium ion balance under salt stress (Fig. 7G, H).

Discussion

The impact of abiotic stress on plant growth varies depending on its intensity, duration, species, and developmental stage. A reduction in biomass is a well-established indicator of stress severity and plant tolerance [64]. Salt stress commonly limits cell expansion and division due to osmotic stress, ion toxicity, and oxidative damage, leading to reduced biomass production [65, 66]. In our study, NaCl significantly reduced shoot and root biomass in both GF677 and GN15, though GF677 consistently maintained higher values across all salinity levels (Fig. 1A–H). These results are in line with previous studies reporting biomass reductions under salt stress in almond [44, 67], grapevine [68, 69], pomegranate [70], olive [71], apple [72], citrus [73], and kiwifruit [74].

However, silicon application—particularly at 2 mM—significantly enhanced biomass accumulation in both GF677 and GN15 under salt stress. This improvement suggests that silicon mitigated salinity-induced damage by supporting key physiological functions such as water retention, nutrient uptake, and metabolic activity. Biomass accumulation under stress is a reliable indicator of plant resilience. The increased shoot and root dry weight in Si-treated plants points to better osmotic adjustment, reduced Na⁺ toxicity, and sustained photosynthetic performance. Additionally, enhanced antioxidant defense likely contributed to reduced oxidative damage and preserved cellular integrity, enabling continued growth under salinity [75–77]. These findings underscore silicon's protective role, consistent with similar reports in tomato [78], mango [79], and *Acacia gerrardii* [80].

These findings indicate that exogenous silicon application effectively alleviates NaCl-induced growth inhibition, thereby enhancing the salinity tolerance of GF677 and GN15 rootstocks. The positive effects of silicon under salinity stress are largely attributed to its role in improving key physiological processes such as photosynthesis, redox homeostasis, and nutrient balance [81]. Furthermore, silicon supports better water relations, hormonal regulation, and root development, all of which contribute to increased biomass accumulation under stress conditions [81, 82]. Among these, hormonal regulation is particularly critical in integrating growth and stress signals. Salinity typically suppresses growth by reducing levels of growth-promoting hormones such as

auxins (IAA), cytokinins, and gibberellins, while elevating stress hormones like abscisic acid (ABA) and ethylene. Silicon has been shown to modulate this hormonal imbalance by sustaining higher levels of IAA and cytokinins under salinity, thereby promoting cell division, root elongation, and shoot development. It may also attenuate ABA overaccumulation, helping to maintain stomatal function and photosynthetic efficiency. These hormonal adjustments enhance root–shoot coordination and cell expansion, ultimately contributing to the increased biomass observed in Si-treated plants—likely reflecting, in part, a silicon-induced improvement in hormonal homeostasis [83, 84].

Leaf relative water content is a key indicator of plant water status and metabolic activity [85]. Salinity stress typically reduces RWC, impairing physiological functions, damaging organelles, and limiting growth [86]. In this study, 50 and 100 mM NaCl significantly reduced RWC, while silicon at 1 and 2 mM effectively alleviated this decline, enhancing water retention (Fig. 2A). Similar reductions under salt stress have been reported in grapevine [69], olive [87], pomegranate [70], pistachio [88], and citrus [89]. This decline mainly results from impaired water uptake, which disrupts the balance between absorption and transpiration, reducing leaf hydration [90].

The observed increase in RWC in silicon-treated plants under NaCl stress can be reasonably attributed to the interplay of several physiological mechanisms. Although we did not directly assess root hydraulic conductivity or aquaporin activity, the significant reduction in Na⁺ accumulation and the enhancement of osmolyte levels—particularly proline, glycine betaine, and soluble sugars—strongly indicate improved osmotic adjustment in Si-supplemented plants. This enhanced osmotic regulation likely facilitated better water retention and uptake under salt stress. Additionally, the decline in electrolyte leakage, malondialdehyde, and hydrogen peroxide levels further supports the notion that Si mitigated membrane damage and preserved cellular integrity. These factors collectively suggest that silicon's role in enhancing cellular integrity, improving osmotic adjustment, and maintaining water uptake under salt stress contributed significantly to the improved RWC observed in this study [91–93].

Under salt stress, excessive accumulation of ROS leads to lipid peroxidation, damaging membrane integrity and increasing K⁺ ion loss from cells [94]. Na⁺ competes with K⁺ for binding sites on the cell membrane, resulting in electrolyte leakage [95, 96]. Lipid peroxidation, indicated by elevated MDA levels, is a hallmark of oxidative stress under NaCl [97, 98]. Our results show that GN15 rootstock suffered greater membrane damage under NaCl stress compared to GF677, with higher electrolyte

leakage, MDA accumulation, and hydrogen peroxide levels. However, silicon supplementation—particularly at 2 mM—significantly mitigated stress-induced damage in both rootstocks. GF677 exhibited a greater reduction in stress markers under Si treatment, suggesting its inherent stress tolerance is further enhanced by silicon application (Fig. 2B–E).

These results are consistent with findings in grapevine [69], walnut [99], pomegranate [70], and orange [100]. The higher MDA levels in GN15 likely reflect greater lipid peroxidation due to weaker antioxidant defenses under NaCl stress. Silicon reduces oxidative damage by boosting both enzymatic and non-enzymatic antioxidants, thereby lowering MDA and ROS accumulation [101]. It also helps preserve membrane integrity by limiting Na⁺ uptake, reinforcing cell walls, and reducing ROS levels [102]. The observed decline in ion leakage and MDA in Si-treated plants supports the role of enhanced antioxidant activity, in agreement with reports in apple [29], *Rosa hybrida* [103], *Glycyrrhiza uralensis* [104], and pepper [105].

Osmoprotectants like soluble proteins, proline, and free amino acids are vital for stress tolerance. In this study, NaCl stress increased osmolyte accumulation in both rootstocks. GN15 showed a 1.9-fold rise in proline at 100 mM NaCl, indicating stronger osmotic adjustment (Fig. 3A, B). Interestingly, silicon reduced proline levels, possibly reflecting stress alleviation, though the mechanism remains unclear. NaCl also elevated soluble sugars, particularly in GN15, with the highest levels at 100 mM NaCl. Silicon, especially at 2 mM, moderated this accumulation, suggesting a role in regulating sugar metabolism under stress (Fig. 3C).

Glycine betaine levels rose under salinity, with GF677 showing higher accumulation (3.3-fold) than GN15 (2.8-fold), indicating more effective osmotic regulation. Silicon further boosted glycine betaine under both control and stress conditions, peaking at 2 mM Si (Fig. 3D). Total soluble protein increased under moderate NaCl (50 mM), especially in GF677, but declined under severe stress (100 mM), particularly in GN15. Silicon, notably at 2 mM, mitigated this decline and maintained higher protein levels, especially in GF677 (Fig. 3E), suggesting a protective role in protein stability under stress.

Proline accumulation under salt stress is a well-known response aiding in oxidative stress mitigation [106]. Shahvali et al. [30] reported peak proline levels in GF677 under high salinity, while Acharya et al. [107] observed a sharp increase in the salt-sensitive Nemaguard but only a mild rise in the tolerant Rootpac 40. In this study, silicon reduced proline levels under salt stress in both rootstocks. Since elevated proline often reflects stress severity, this reduction suggests that silicon alleviates salt-induced damage [108].

Salt stress caused a notable increase in soluble sugars in both GF677 and GN15 rootstocks, consistent with previous findings in almond, grapevine, and tomato [44, 69, 109, 110]. Soluble sugars not only help maintain osmotic balance but also serve as immediate energy sources for stress metabolism and act as important signaling molecules regulating stress-responsive genes. For instance, hexokinase-dependent sugar signaling pathways influence antioxidant defenses and growth under abiotic stress. In our study, silicon application—especially at 2 mM—significantly reduced the salt-induced sugar accumulation, suggesting it helps restore sugar homeostasis. This effect might be linked to enhanced phloem loading and sugar translocation from leaves to roots, as reported by Zhu [17]. Additionally, silicon may modulate sugar signaling by affecting enzymes such as invertases and sucrose transporters or by altering hexokinase-mediated pathways. These findings suggest that silicon plays a role in balancing carbon allocation between osmotic protection, energy supply, and signaling during salt stress. However, further molecular research is needed to uncover the precise mechanisms involved [76, 111, 112].

Glycine betaine, an important organic osmolyte, helps plants maintain osmotic balance by reducing cellular water loss and scavenging reactive oxygen species (ROS), thereby protecting proteins from salt-induced oxidative damage [113, 114]. In line with our results, previous studies in *citrus* rootstocks showed that salt stress increases glycine betaine levels in both leaves and roots, with tolerant rootstocks accumulating more than sensitive ones [115]. Moreover, silicon treatment enhanced glycine betaine content under both control and salt stress conditions, supporting the findings of Al-Huqail et al. [80], and El Moukhtari et al. [101].

Protein synthesis, a key indicator of a plant's biochemical state, is often impaired by salinity stress. Consistent with our findings, 40 mM NaCl increased soluble protein levels in the leaves of wild almond rootstocks [116]. Research shows that silicon application under salt stress can enhance protein content by reducing stress-induced damage, supporting enzymatic function and stress-related metabolism. Additionally, silicon may stabilize proteins by improving nutrient transport, lowering ROS levels, and boosting antioxidant defenses [84, 117, 118].

Our results show that NaCl stress significantly increased antioxidant enzyme activities in both rootstocks, with GF677 displaying a stronger response than GN15 (Fig. 4A–G). This suggests that GF677 has a more effective enzymatic defense against salt stress. Moreover, silicon—especially at 2 mM—further enhanced antioxidant activity, likely contributing to reduced oxidative damage. Enhanced antioxidant enzyme activity is a key mechanism of salt stress tolerance in plants [119]. Amani et al. [67] reported increased SOD, CAT, POD, and APX

activity in two almond cultivars grafted onto GF677 under salinity. Similarly, Hatami et al. [120] observed elevated CAT and POD activity in GF677, GN15, and bitter almond, while Tavallali and Karimi [45] found stronger enzymatic responses in GF677 compared to bitter almond. Our findings confirm that silicon further enhances antioxidant enzyme activity, supporting its role in mitigating oxidative stress. Silicon likely contributes to ROS detoxification by regulating antioxidant enzymes, although its effects may differ across species [121]. This is consistent with reports in *Arabidopsis* [122], cucumber [123], sweet pepper [105], roses [103], and tomato [124]. Key limiting factors in the light-dependent phase of photosynthesis under salinity include reduced carbon fixation enzyme activity [125], damage to the photosynthetic apparatus [126], decreased pigments, and impaired electron transport between photosystems II and I [127]. ROS-induced degradation of the D1 protein also disrupts PSII repair. Notably, carbon fixation is more sensitive to salt stress than light reactions [128]. Salinity primarily causes osmotic stress, leading to stomatal closure and reduced CO₂ availability, which limits carbon fixation. Beyond stomatal effects, salinity also impairs light-dependent reactions, further reducing plant performance [129]. In this study, NaCl significantly decreased net photosynthesis (Pn) and stomatal conductance in both rootstocks, with GN15 showing a sharper decline. However, 2 mM Si alleviated these effects, maintaining higher Pn levels (Fig. 5A–D).

Sandhu et al. [130] reported that salinity reduced photosynthetic rates in 14 almond rootstocks. Similarly, Hatami et al. [120] reported that salinity stress noticeably reduced photosynthesis, stomatal conductance, and transpiration in both rootstocks, with GN15 showing a greater sensitivity compared to GF677. These findings, consistent with our results, indicate that GF677 undergoes a less severe reduction in gas exchange under salt stress, reflecting its greater tolerance compared to GN15. The partial recovery of photosynthetic rate (Pn) and stomatal conductance (gs) in silicon-treated plants under salt stress—especially at 2 mM Si—can be linked to physiological effects observed in our study. Silicon improved ion homeostasis by reducing Na⁺ accumulation and enhancing K⁺ retention (Fig. 6), which helps maintain osmotic balance and turgor pressure in guard cells. This prevents excessive stomatal closure, supporting higher gs values (Fig. 5C, D) and facilitating greater CO₂ uptake, contributing to the improved Pn (Fig. 5A, B).

Moreover, silicon's protective role in maintaining membrane integrity and boosting antioxidant defenses, as shown by our results, likely helps preserve photosynthetic function under salt-induced oxidative stress. These combined physiological effects explain the improved Pn and gs observed in Si-treated plants under both moderate

and severe salinity. This enhancement in gas exchange led us to further investigate how silicon influences stomatal behavior and its impact on photosynthetic efficiency under salinity.

The reduction in stomatal conductance under increasing salinity in both rootstocks likely reflects stomatal closure to reduce water loss. However, this also limits CO₂ entry, contributing to the decline in photosynthetic rate under salt stress (Fig. 5A–D). The close link between reduced gs and Pn highlights how sensitive gas exchange is to stomatal limitations caused by salinity. Notably, silicon treatment partially restored gs, suggesting silicon helps maintain stomatal function during salt stress. This effect may result from improved osmotic regulation and decreased ionic toxicity, evidenced by higher K⁺ retention and lower Na⁺ accumulation (Fig. 6). These improvements likely sustain leaf water status, delay stomatal closure, and support better CO₂ uptake, thereby enhancing photosynthesis. Overall, these results reveal a key role for silicon in preserving photosynthetic efficiency under saline conditions [104, 111, 131].

Silicon alleviates salinity stress by reducing ion toxicity and limiting ROS accumulation, which helps preserve the function and structure of photosynthetic organelles. It also enhances stomatal conductance, maintains photosynthetic pigment levels, and improves photosystem II efficiency, resulting in increased photosynthesis and better plant growth under stress conditions [85]. Furthermore, silicon's role in salinity tolerance involves the regulation of aquaporins, phytohormones, polyamines, and ion transport genes. Enhanced aquaporin activity boosts root hydraulic conductance, supporting stomatal function and sustaining photosynthesis during salt stress [132, 133].

Salinity stress causes ionic toxicity by leading to excessive Na⁺ and Cl⁻ accumulation in plant cells, disrupting the Na⁺/K⁺ balance and impairing growth. Its harmful effects arise from osmotic stress, ion overload cytotoxicity, nutrient imbalances, and reduced turgor pressure [134, 135]. In this study, NaCl stress significantly increased Na⁺ and Cl⁻ levels in both roots and leaves of GF677 and GN15, with the highest accumulation at 100 mM NaCl. GN15 accumulated more Na⁺ than GF677, especially under severe salinity. Silicon supplementation, particularly at 2 mM, effectively reduced Na⁺ and Cl⁻ uptake, highlighting its role in mitigating salt stress and maintaining ionic balance. Potassium levels decreased with salinity, but GF677 retained higher K⁺ than GN15 at both 50 and 100 mM NaCl. Silicon helped sustain K⁺ concentrations in roots and leaves, with the greatest effect at 2 mM under severe salinity. Silicon uptake also increased, especially in roots, further supporting its protective function. These results underscore the importance of silicon at 2 mM in improving ionic homeostasis,

with GN15 showing higher ion accumulation but benefiting from silicon treatment (Fig. 6A–N).

Salt stress disrupts nutrient balance because Na^+ and K^+ have similar hydrated radii, making it difficult for membrane transporters to distinguish between them, which leads to Na^+ toxicity under high salinity [136]. Na^+ can enter cells via K^+ transporters [137], and excessive Na^+ accumulation causes K^+ leakage [102], becoming especially harmful above 50 mM NaCl in both rootstocks. Additionally, K^+ channels may inadvertently allow Na^+ influx during salt stress, worsening ion toxicity [138]. Silicic acid moves through the xylem to upper plant parts via transpiration, where it is deposited as insoluble hydrated silica in the apoplastic spaces of stems and leaves [139, 140].

This silica forms a barrier in the apoplast that limits Na^+ transport [141]. Moreover, silicon promotes the development of the Casparian strip in the root exodermis and endodermis, further preventing Na^+ entry via the apoplast [142]. Shao et al. [143] found a strong correlation between increased suberin and lignin deposition and salt tolerance in almond rootstocks. Notably, the E1 almond rootstock showed greater salt tolerance by enhancing suberin and lignin accumulation in root exodermis and endodermis under salinity stress, creating a barrier that restricts apoplastic Na^+ transport.

The expression patterns of key salt-responsive genes—including *HKT1*, *NHX1*, *AVP1*, and *SOS1*—demonstrate distinct tissue-specific roles that are crucial for maintaining ion homeostasis under saline conditions (Fig. 7A–H). In our study, *HKT1* was predominantly upregulated in the roots of GF677, particularly under silicon treatment. This pattern is consistent with findings by Kaundal et al. [144], who reported root-specific *HKT1* expression in almond as a mechanism to retrieve Na^+ from the xylem, thereby limiting its translocation to shoots. Similarly, Sandhu et al. [130] observed elevated *HKT1* expression in the roots of Empyrean1 rootstock under salt stress. These parallels suggest that *HKT1* upregulation in GF677 roots plays a pivotal role in minimizing Na^+ accumulation in the shoot, protecting photosynthetically active tissues from ion toxicity. Our data extend these insights by showing that silicon further amplifies this gene expression, strengthening root-mediated Na^+ exclusion.

In contrast, *NHX1* and *AVP1* were most strongly expressed in leaves, where they contribute to vacuolar Na^+ sequestration—an essential mechanism for maintaining cytosolic ion balance [145, 146]. This leaf-specific expression is particularly important for preserving cellular function in photosynthetic tissues, where Na^+ toxicity can directly impair metabolic processes such as photosynthesis. Our results align with those of Li et al. [147], who also reported leaf-localized expression of these genes in apple under salt stress. We observed that silicon

enhances this leaf-based sequestration strategy in GF677, likely improving photosynthetic efficiency by facilitating vacuolar compartmentalization of excess Na^+ . The root-specific expression of *SOS1*, which promotes Na^+ efflux from root cells into the rhizosphere, was also significantly upregulated in response to silicon. This supports earlier work by Amani et al. [67] in almond, and underscores the importance of active Na^+ exclusion at the root-soil interface. By enhancing *SOS1* expression, silicon appears to synergize with intrinsic salt-tolerance pathways to prevent systemic Na^+ overload. Collectively, these findings highlight the tissue-specific coordination of gene expression in response to salinity stress. Roots primarily serve as a barrier against Na^+ entry (*HKT1*, *SOS1*), while leaves function as detoxification sites via vacuolar sequestration (*NHX1*, *AVP1*). Silicon appears to fine-tune both processes, reinforcing the functional differentiation between tissues and amplifying plant resilience to salinity. Rather than merely echoing previous literature, our results integrate and extend these mechanistic insights by demonstrating how silicon modulates gene expression in a spatially distinct manner to optimize salt tolerance in GF677.

Conclusion

This study highlights the significant role of silicon in mitigating the adverse effects of NaCl stress on GF677 and GN15 rootstocks, particularly under moderate to high NaCl concentrations. Silicon supplementation, especially at 2 mM, enhanced plant growth, water retention, and biomass accumulation while reducing oxidative damage by decreasing electrolyte leakage, lipid peroxidation, and hydrogen peroxide levels. Additionally, silicon improved the accumulation of compatible osmolytes such as proline, soluble sugars, glycine betaine, and total soluble proteins, contributing to enhanced stress tolerance. The results also revealed that silicon application modulated gene expression associated with salt tolerance, including genes like *HKT1*, *AVP1*, *NHX1*, and *SOS1*, with a more pronounced effect observed in GF677 rootstocks. Silicon treatment further promoted antioxidant enzyme activities, providing additional protection against salinity-induced oxidative stress. Furthermore, silicon supplementation reduced Na^+ and Cl^- accumulation in both leaves and roots, maintaining ionic balance and mitigating salt toxicity.

In conclusion, our findings suggest that silicon is an effective ameliorator of NaCl-induced stress, improving salt tolerance in both rootstocks, particularly GF677. These results indicate that silicon may serve as a useful tool in agricultural practices aimed at enhancing plant resilience to salinity. To translate these findings into practical applications, future research should focus on testing silicon supplementation under real-field conditions

across diverse agricultural environments and varying salinity levels. Furthermore, long-term impacts on soil health, nutrient cycling, and crop yield should be explored. It will also be important to determine optimal silicon concentrations for different crops and soil types. Future challenges include scaling up silicon use in large-scale farming systems, managing cost-effectiveness, and ensuring consistent outcomes under variable environmental conditions. Overall, integrating silicon into salinity management strategies may contribute to improved crop productivity and agricultural sustainability, especially in salt-affected region.

Abbreviations

LRWC	Leaf relative water content
Pn	Net photosynthesis
H ₂ O ₂	Hydrogen peroxide
MDA	Malondialdehyde
EL	Electrolyte leakage
SOD	Superoxide dismutase
GPX	Guaiacol peroxidase
CAT	Catalase
GPX	Guaiacol peroxidase
APX	Ascorbate-peroxidase
ROS	Reactive Oxygen Species
Si	Silicon
Na ⁺	Sodium
K ⁺	potassium
Cl ⁻	Chloride
EDTA	Ethylenediaminetetraacetic acid
BSA	bovine serum albumin
PCR	Polymerase chain reaction
NTC	No-template control
cDNA	complementary DNA

Acknowledgements

The authors of this article would like to thank all the staff of Horticultural Science Department of Urmia University, Faculty of Agriculture.

Author contributions

P., J., and M., conceived and designed the experiments, wrote, edited, and analyzed the data and conducted the experiments. L., and N., read and edited the manuscript. All authors have read the paper and have approved the final manuscript.

Funding

No funding was received for this work.

Data availability

The datasets used in this paper are available from the first author on reasonable request.

Declarations

Ethics approval and consent to participate

Not applicable.

Consent for publication

Not applicable.

Competing interests

The authors declare no competing interests.

Author details

¹Department of Horticultural Science, Faculty of Agriculture, Urmia University, Urmia, Iran

²Department of Horticultural Sciences, Faculty of Agriculture, University of Tabriz, Tabriz, Iran

³Department of Soil Science, Faculty of Agriculture, Urmia University, Urmia, Iran

Received: 13 April 2025 / Accepted: 20 May 2025

Published online: 28 May 2025

References

- Rachappanavar V, Kumar M, Negi N, Chowdhury S, Kapoor M, Singh S, Yadav AN. Silicon derived benefits to combat biotic and abiotic stresses in fruit crops: current research and future challenges. *Plant Physiol Biochem*. 2024;108680. <https://doi.org/10.1016/j.plaphy.2024.108680>.
- Ouhibi C, Attia H, Rebah F, Msilini N, Chebbi M, Aarouf J. Salt stress mitigation by seed priming with UV-C in lettuce plants: growth, antioxidant activity and phenolic compounds. *Plant Physiol Biochem*. 2014;83:126–33. <https://doi.org/10.1016/j.plaphy.2014.07.019>.
- Zhang JL, Zhang JZ, Shen JB, Tian J, Jin KM, Zhang FS. Soil health and agriculture green development: opportunities and challenges. *Acta Pedol Sin*. 2020;57:783–96. <https://doi.org/10.11766/trxb202002220064>.
- Hasanuzzaman M, Nahar K, Alam MM, Bhowmik PC, Hossain MA, Rahman MM, Prasad MNV, Ozturk M, Fujita M. Potential use of halophytes to remediate saline soils. *BioMed Res Int*. 2014;1:589341. <https://doi.org/10.1155/2014/589341>.
- Hossain MS. Present scenario of global salt affected soils, its management and importance of salinity research. *Int J Biol Sci*. 2019;1:1–3.
- Dabravolski SA, Isayenkov SV. The physiological and molecular mechanisms of silicon action in salt stress amelioration. *Plants*. 2024;13(4):525. <https://doi.org/10.3390/plants13040525>.
- Balasubramaniam T, Shen G, Esmaeili N, Zhang H. Plants response mechanisms to salinity stress. *Plants*. 2023;12(12):2253. <https://doi.org/10.3390/plants12122253>.
- Assaha DVM, Ueda A, Saneoka H, Al-Yahyai R, Yaish MW. The role of Na⁺ K⁺ Transporters Salt Stress Adaptation Glycophytes *Front Physiol*. 2017;8:509. <https://doi.org/10.3389/fphys.2017.00509>.
- Kibria MG, Hoque MD. A review on plant responses to soil salinity and amelioration strategies. *J Soil Sci*. 2019;9:219–31. <https://doi.org/10.4236/ojss.2019.911013>.
- Xiao F, Zhou H. Plant salt response: perception, signaling, and tolerance. *Front Plant Sci*. 2023;13:1053699. <https://doi.org/10.3389/fpls.2022.1053699>.
- Venturas MD, Sperry JS, Hacke UG. Plant xylem hydraulics: what we understand, current research, and future challenges. *J Plant Biol*. 2017;59(6):356–89. <https://doi.org/10.1111/jipb.12534>.
- Shahid MA, Sarkhosh A, Khan N, Balal RM, Ali Sh, Rossi L, Gómez C, Mattson N, Nasim W, Garcia-Sanchez F. Insights into the physiological and biochemical impacts of salt stress on plant growth and development. *Agron*. 2020;10(938):1–34. <https://doi.org/10.3390/agronomy10070938>.
- Munns R, James RA, Läuchli A. Approaches to increasing the salt tolerance of wheat and other cereals. *J Exp Bot*. 2006;57(5):1025–43. <https://doi.org/10.1093/jxb/erj100>.
- Yamaguchi Nakhoda B, Leung HT, Mendiolo M, Nejad GM, Ismail AM. Isolation, characterization, and field evaluation of rice (*Oryza sativa* L., Var. IR64) mutants with altered responses to salt stress. *Field Crops Res*. 2012;127:191–202. <https://doi.org/10.1016/j.fcr.2011.11.004>.
- Schilling RK, Tester M, Marschner P, Plett DC, Roy SJ. AVP1: one protein, many roles. *Trends Plant Sci*. 2017;22(2):154–62. <https://doi.org/10.1016/j.tplants.2016.11.012>.
- Shi H, Quintero FJ, Pardo JM, Zhu JK. The putative plasma membrane Na⁺/H⁺ antiporter SOS1 controls long-distance Na⁺ transport in plants. *Plant Cell*. 2002;14:465–77. <https://doi.org/10.1105/tpc.010371>.
- Zhu JK. Abiotic stress signaling and responses in plants. *Cell*. 2016;167:313–24. <https://doi.org/10.1016/j.cell.2016.08.029>.
- Meena VD, Dotaniya ML, Coumar V, Rajendiran S, Ajay Kundu S, Subba Rao A. A case for silicon fertilization to improve crop yields in tropical soils. *Proc Natl Acad Sci India Sect B Biol Sci*. 2014;84:505–18. <https://doi.org/10.1007/s40011-013-0270-y>.
- Savvas D, Ntatsi G. Biostimulant activity of silicon in horticulture. *Sci Hortic*. 2015; 196: 66–81. <https://doi.org/10.1016/j.scienta.2015.09.010>
- Dogan M, Bolat I, Turan M, Kaya O. Elucidating stress responses in *Prunus* rootstocks through comprehensive evaluation under drought, heat shock

- and combined stress conditions. *Sci Hortic.* 2025;339(1):113882. <https://doi.org/10.1016/j.scienta.2024.113882>.
21. de Mello Prado R, Alves DMR, de Soares AVL A. Silicon: the only element in plant nutrition with a mitigating effect on multiple stresses. In: de Mello Prado R, Etesami H, Srivastava AK, editors. *Silicon advances for sustainable agriculture and human health. sustainable plant nutrition in a changing world*. Cham: Springer; 2024. https://doi.org/10.1007/978-3-031-69876-7_2.
 22. Wang S, Shen X, Guan X, Sun L, Yang Z, Wang D, Chen Y, Li P, Xie Z. Nano-silicon enhances tomato growth and antioxidant defense under salt stress. *Environmental science. NANO.* 2024;12(1). <https://doi.org/10.1039/D4EN00770K>.
 23. Hafez EM, Osman HS, Gawayed SM, Okasha SA, Omara AED, Sami R. Minimizing the adversely impacts of water deficit and soil salinity on maize growth and productivity in response to the application of plant growth-promoting rhizobacteria and silica nanoparticles. *Agronomy.* 2021;11:676. <https://doi.org/10.3390/agronomy11040676>.
 24. Elsheery NJ, Helaly MN, El-Hoseiny HM, Alam-Eldein SM. Zinc oxide and silicone nanoparticles to improve the resistance mechanism and annual productivity of salt-stressed Mango trees. *Agron.* 2020;10:558. <https://doi.org/10.3390/agronomy10040558>.
 25. Fahad S, Hussain S, Matloob A, Khan FA, Khaliq A, Saud S, Huang J. Phytohormones and plant responses to salinity stress: a review. *Plant Growth Regul.* 2015;75:391–404. <https://doi.org/10.1007/s10725-014-0013-y>.
 26. Liu YongXia LY, Xu L, XiZeng XX. Effects of silicon on polyamine types and forms in leaf of *Zizyphus jujube* Cv. Jinsi-xiaozao under salt stress. *J Nanjing Univ.* 2007;31:27–32.
 27. Kim YH, Khan AL, Waqas M, Lee IJ. Silicon regulates antioxidant activities of crop plants under abiotic-induced oxidative stress: a review. *Front Plant Sci.* 2017;8:510. <https://doi.org/10.3389/fpls.2017.00510>.
 28. Aras S. Silicon nutrition in alleviating salt stress in Apple plant. *Acta Sci Pol-Hortoru.* 2020;19(1):3–10. <https://doi.org/10.24326/asphc.2020.1.1>.
 29. Qin L, Kang Wh, Qi YL, Zhang ZW, Wang N. The influence of silicon application on growth and photosynthesis response of salt stressed grapevines (*Vitis vinifera* L.). *Acta Physiol Plant.* 2016;38:68. <https://doi.org/10.1007/s11738-016-2087-9>.
 30. Shahvali R, Shiran B, Ravash R, Fallahi B, Hanović Đeri B. Effect of symbiosis with arbuscular mycorrhizal fungi on salt stress tolerance in GF677 (peach x almond) rootstock. *Sci Hortic.* 2020;272:109535. <https://doi.org/10.1016/j.scienta.2020.109535>.
 31. Zhang D, Zhang Z, Wang Y. Effects of salt stress on salt-repellent and salt-secreting characteristics of two Apple rootstocks. *Plants.* 2024;13(7):1046. <https://doi.org/10.3390/plants13071046>.
 32. Felipe AJ, Felinim, Garnem, and Monegro almond *peach hybrid rootstocks. *HortScience.* 2009;44:196–7. <https://doi.org/10.21273/HORTSCI.44.1.196>.
 33. Momenpour A, Imani A, Bakhshi D, Akbarpour E. Evaluation of salinity tolerance of some selected almond genotypes budded on GF 677 rootstock. *Int J Fruit Sci.* 2018;18(1):1–26. <https://doi.org/10.1080/15538362.2018.1468850>.
 34. Aras S, Eşitken A, Karakurt Y. The comprehensive responses of young sweet Cherry trees under moderate saline conditions depending on the different rootstocks. *Erwerbs-Obstbau.* 2023;1–9. <https://doi.org/10.1007/s10341-023-00838-3>.
 35. Papadakis IE, Veneti G, Chatzissavvidis C, Therios I. Physiological and growth responses of sour Cherry (*Prunus cerasus* L.) plants subjected to short-term salinity stress. *Acta Bot Croat.* 2018;77(2):197–202.
 36. Al-Saif AM, Abdrabbob GA, Abdel-Aziz HF, Abd A, Elnaggar IA, Abd EI AEWN, Hamdy AE. Uncovering of some citrus rootstocks to salt stress tolerance in vitro screening. 2023; 2023071216. <https://doi.org/10.20944/preprints202307.1216.v1>
 37. Etesami H, Jeong BR. Silicon (Si): review and future prospects on the action mechanisms in alleviating biotic and abiotic stresses in plants. *Ecotoxic Environ Saf.* 2018;147:881–96.
 38. Tayade R, Ghimire A, Khan W, Lay L, Attipoe JQ, Kim Y. Silicon as a smart fertilizer for sustainability and crop improvement. *Biomolecules.* 2022;12(8):1027. <https://doi.org/10.3390/biom12081027>.
 39. Mozafari AA, Ghadakchi asl A, Ghaderi N. Grape response to salinity stress and role of iron nanoparticle and potassium silicate to mitigate salt induced damage under in vitro conditions. *Physiol Mol Biol Plants.* 2018;24:25–35. <https://doi.org/10.1007/s12298-017-0488-x>.
 40. Mahmoud LM, Dutt M, Shalan AM, El-Kady ME, El-Boray MS, Shabana YM, Grosser JW. Silicon nanoparticles mitigate oxidative stress of in vitro-derived banana (*Musa acuminata* 'grand Nain') under simulated water deficit or salinity stress. *S Afr J Bot.* 2020;132:155–63. <https://doi.org/10.1016/j.sajb.2020.04.027>.
 41. Sohby MK, Khalil HA, Eissa AM, Fekry WM. Influence of nano-silicon and nano-chitosan on growth, ion, content, and antioxidant defense enzyme of two citrus rootstocks under salinity conditions. *Mesop J Agric.* 2023;51(2):147–66. <https://doi.org/10.33899/magrij.2023.179915>.
 42. Kılıç M, Arslan E, Eşitken A. Silicon increased sodium transporter gene expressions in Apple under short- and long-term salt stress. *Erwerbs-Obstbau.* 2023;65(3):419–22. <https://doi.org/10.1007/s10341-023-00848-1>.
 43. Bolat I, Bakır AG, Korkmaz K, Gutiérrez-Gamboa G, Kaya O. Silicon and nitric oxide applications allow mitigation of water stress in Myrobalan 29 C rootstocks (*Prunus cerasifera* Ehrh). *Agriculture.* 2022;12(8):1273. <https://doi.org/10.3390/agriculture12081273>.
 44. Aazami MA, Rasouli F, Panahi Tajaragh R. Influence of salinity stress on morphological, nutritional and physiological attributes in different cultivars of *Prunus amygdalus* L. *J Plant Nut.* 2021;12(44):1758–69. <https://doi.org/10.1080/01904167.2021.1881549>.
 45. Tavallali V, Karimi S. Methyl jasmonate enhances salt tolerance of almond rootstocks by regulating endogenous phytohormones, antioxidant activity and gas-exchange. *J Plant Physiol.* 2019;234–235:98–105. <https://doi.org/10.1016/j.jplph.2019.02.001>.
 46. Hoagland DR, Arnon DI. The water-culture method for growing plants without soil. Circular. California agricultural experiment station. 1950; 347(2nd edit).
 47. Ritchie JC, McHenry JR. Application of radioactive fallout cesium 137 for measuring soil erosion and sediment accumulation rates and patterns: A review. *J Environ Qual.* 1990;19(2):215–33. <https://doi.org/10.2134/jeq1990.0047242501900020006x>.
 48. Lutts S, Kinet JM, Bouharmont J. NaCl-induced senescence in leaves of rice (*Oryza sativa* L.) cultivars differing in salinity resistance. *Ann Bot.* 1996;78(3):389–98. <https://doi.org/10.1006/anbo.1996.0134>.
 49. Velikova V, Yordanov I, Edreva AJPS. Oxidative stress and some antioxidant systems in acid rain-treated bean plants: protective role of exogenous polyamines. *Plant Sci.* 2000;151(1):59–66. [https://doi.org/10.1016/S0168-9452\(99\)00197-1](https://doi.org/10.1016/S0168-9452(99)00197-1).
 50. Cakmak I, Horst WJ. Effect of aluminium on lipid peroxidation, superoxide dismutase, catalase, and peroxidase activities in root tips of soybean (*Glycine max*). *Physiol Plant.* 1991;83(3):463–8. <https://doi.org/10.1111/j.1399-3054.1991.tb00121.x>.
 51. Haworth M, Marino G, Centritto M. An introductory guide to gas exchange analysis of photosynthesis and its application to plant phenotyping and precision irrigation to enhance water use efficiency. *J Water Clim Chang.* 2018;9(4):786–808. <https://doi.org/10.2166/wcc.2018.152>.
 52. Irigoyen JJ, Einerich DW, Sánchez-Díaz M. Water stress induced changes in concentrations of proline and total soluble sugars in nodulated alfalfa (*Medicago sativa*) plants. *Physiol Plant.* 1992;84(1):55–60. <https://doi.org/10.1111/j.1399-3054.1992.tb08764.x>.
 53. Grieve CM, Grattan SR. Rapid assay for determination of water soluble quaternary ammonium compounds. *Plant Soil.* 1983;70:303–7. <https://doi.org/10.1007/BF02374789>.
 54. Bradford MM. A rapid and sensitive method for the quantitation of microgram quantities of protein utilizing the principle of protein-dye binding. *Anal Biochem.* 1976;72(1–2):248–54. [https://doi.org/10.1016/0003-2697\(76\)90527-3](https://doi.org/10.1016/0003-2697(76)90527-3).
 55. Kang HM, Saltveit ME. Chilling tolerance of maize, cucumber and rice seedling leaves and roots are differentially affected by Salicylic acid. *Physiol Plant.* 2002;115(4):571–6. <https://doi.org/10.1034/j.1399-3054.2002.1150411.x>.
 56. Aebi H. Catalase in vitro. In *Methods in enzymology*. 1984; 105: 121–126. Academic press. [https://doi.org/10.1016/S0076-6879\(84\)05016-3](https://doi.org/10.1016/S0076-6879(84)05016-3)
 57. Upadhyaya A, Sankhla D, Davis TD, Sankhla N, Smith BN. Effect of Paclobutrazol on the activities of some enzymes of activated oxygen metabolism and lipid peroxidation in senescing soybean leaves. *J Plant Physiol.* 1985;121(5):453–61. [https://doi.org/10.1016/S0176-1617\(85\)80081-X](https://doi.org/10.1016/S0176-1617(85)80081-X).
 58. Nakano Y, Asada K. Hydrogen peroxide is scavenged by ascorbate specific peroxidase in spinach chloroplasts. *J Plant Cell Physiol.* 1981;22:867–80. <https://doi.org/10.1093/oxfordjournals.pcp.a076232>.
 59. Beauchamp CO, Fridovich I. Isozymes of superoxide dismutase from wheat germ. *Biochim Biophys Acta Protein Struct.* 1973;317(1):50–64. [https://doi.org/10.1016/0005-2795\(73\)90198-0](https://doi.org/10.1016/0005-2795(73)90198-0).
 60. Mizukoshi K, Nishiwaki T, Ohtake N, Minagawa R, Kobayashi K, Ikarashi T, Ohshima T. Determination of tungstate concentration in plant materials by

- HNO₃-HC1 O₄ digestion and colorimetric method using thiocyanate. Bulletin Faculty of Agriculture Niigata University. 1994.
61. Amami A. Methods of plant analysis (Number 982). Soil and water research Institute. Agricultural Research, Education and Extension Organization. 1996; (In Persian).
 62. Elliott CL, Snyder GH. Autoclave-induced digestion for the colorimetric determination of silicon in rice straw. J Agric Food Chem. 1991;39(6):1118–9.
 63. Pfaf MW, Tichopad A, Prgomet C, Neuvians TP. Determination of stable house-keeping genes, differentially regulated target genes and sample integrity: BestKeeper–Excel-based tool using pair-wise correlations. Biotechnol Lett. 2004;26(6):509–15. <https://doi.org/10.1023/B:BILE.0000019559.84305.47>.
 64. Sun M, Wang T, Fan L, Wang H, Pan H, Cui X, Lou Y, Zhuge Y. Foliar applications of spermidine improve Foxtail millet seedling characteristics under salt stress. Plant Biol. 2020;64:353–62. <https://doi.org/10.32615/bp.2019.158>.
 65. Zhang M, Fang Y, Ji Y, Jiang Z, Wang L. Effects of salt stress on ion content, antioxidant enzymes and protein profile in different tissues of *Broussonetia papyrifera*. S Afr J Bot. 2013;85:1–9. <https://doi.org/10.1016/j.sajb.2012.11.005>.
 66. Sarker U, Oba S. The response of salinity stress-induced A. tricolor to growth, anatomy, physiology, non-enzymatic and enzymatic antioxidants. Front Plant Sci. 2020;11:559876. <https://doi.org/10.3389/fpls.2020.559876>.
 67. Amani G, Shamili M, Imani A, Mousavi A, Rezai H. Impact of salinity on growth rate, physiology, elemental composition, and *NHX1* gene expression of almond (*Prunus dulcis*) cultivars. J Nuts. 2024;15(1):31–60.
 68. Shokri G, Amiri J, Barin M. Spermidine mitigates salt stress in grapevine with alterations in physicochemical properties and nutrient composition. J Plant Nut Soil Sci. 2024;1–17. <https://doi.org/10.1002/jpln.202400003>.
 69. El-Banna MF, AL-Huqail AA, Farouk S, Belal BEA, El-Kenawy MA, Abd El-Khalek AF. Morpho-physiological and anatomical alterations of salt-affected Thompson seedless grapevine (*Vitis vinifera* L.) to Brassinolide spraying. Horticulture. 2022;8:568. <https://doi.org/10.3390/horticulturae8070568>.
 70. Khalil HA, El-Ansary DO, Ahmed ZF. Mitigation of salinity stress on pomegranate (*Punica granatum* Lcv.Wonderful) plant using Salicylic acid foliar spray. Horticulturae. 2022;8(5):375. <https://doi.org/10.3390/horticulturae8050375>.
 71. Regni L, Delpino AM, Mousavi S, Palmerini CA, Baldoni L, Mariotti R, Mairech H, Gardi T, Proietti P. Behavior of our Olive cultivars during salt stress. Front Plant Sci. 2019;10:436704. <https://doi.org/10.3389/fpls.2019.00867>.
 72. Huo L, Guo Z, Wang P, Zhang Z, Jia X, Sun Y, Sun X, Gong X, Ma F. MdATG8l functions positively in Apple salt tolerance by maintaining photosynthetic ability and increasing the accumulation of arginine and polyamines. Environ Exp Bot. 2020;172:103989. <https://doi.org/10.1016/j.envexpbot.2020.103989>.
 73. Alam A, Ullah H, Attia A, Datta A. Effects of salinity stress on growth, mineral nutrient accumulation and biochemical parameters of seedlings of three citrus rootstocks. Int J Fruit Sci. 2020;20(4):786–804. <https://doi.org/10.1080/15538362.2019.1674762>.
 74. Abid M, Zhang YJ, Li Z, Bai DF, Zhong YP, Fang JB. Effect of salt stress on growth, physiological and biochemical characters of four Kiwifruit genotypes. Sci Hort. 2020;271:109473. <https://doi.org/10.1016/j.scienta.2020.109473>.
 75. Rios JJ, Martínez-Ballesta MC, Ruiz JM, Blasco B, Carvajal M. Silicon-mediated improvement in plant salinity tolerance: the role of Aquaporins. Front Plant Sci. 2017;8:948. <https://doi.org/10.3389/fpls.2017.00948>.
 76. Kumar A, Choudhary A, Kaur H, Singh K, Guha S, Choudhary DR, Sonkar A, Mehta S, Husen A. Exploring the role of silicon in enhancing sustainable plant growth, defense system, environmental stress mitigation and management. Discov Appl Sci. 2025;7:406. <https://doi.org/10.1007/s42452-025-06866-w>.
 77. Saad Ullah M, Mahmood A, Najeib Alawadi HF, Seleiman MF, Ahmad Khan B, Javaid MM, Wahid A, Abdullah F, Wasonga DO. Silicon-mediated modulation of maize growth, metabolic responses, and antioxidant mechanisms under saline conditions. BMC Plant Biol. 2025;25:3. <https://doi.org/10.1186/s12870-024-06013-4>.
 78. Hernández-Salinas M, Valdez-Aguilar LA, Alia-Tejecal I, Alvarado-Camarillo D, Cartmill AD. Silicon enhances the tolerance to moderate NaCl-salinity in tomato grown in a hydroponic recirculating system. J Plant Nutr. 2022;45:3:413–25. <https://doi.org/10.1080/01904167.2021.1963772>.
 79. Doaa MH, Shalan AM. Inducing salinity tolerance in Mango (*Mangifera indica* L.) Cv. El-Gahrawey by sodium silicate pentahydrate and glycine betaine. J Plant Prod. 2020;11(6):541–9. <https://doi.org/10.21608/jpp.2020.106333>.
 80. Al-Huqail AA, Alqarawi AA, Hashem A, Malik JA, Abd Allah EF. Silicon supplementation modulates antioxidant system and osmolyte accumulation to balance salt stress in *Acacia gerrardii* Benth. Saudi J Biol Sci. 2019;26(7):1856–64. <https://doi.org/10.1016/j.sjbs.2017.11.049>.
 81. Liu B, Soundararajan P, Manivannan A. Mechanisms of silicon-mediated amelioration of salt stress in plants. Plants. 2019;8(9):307. <https://doi.org/10.3390/plants8090307>.
 82. Manivannan A, Soundararajan P, Muneer S, Ko CH, Jeong BR. Silicon mitigates salinity stress by regulating the physiology, antioxidant enzyme activities, and protein expression in *Capsicum annuum* Bugwang. BioMed Res Inter. 2016;1–14. <https://doi.org/10.1155/2016/3076357>.
 83. Tian XY, He MR, Wang ZL, Zhang JW, Song YL, He ZL, Dong YJ. Application of nitric oxide and calcium nitrate enhances tolerance of wheat seedlings to salt stress. Plant Growth Regul. 2015;77:343–56. <https://doi.org/10.1007/s10725-015-0069-3>.
 84. Xiong J, Yang X, Sun M, Zhang J, Ding L, Sun Z, Feng N, Zheng D, Zhao L, Shen X. Mitigation effect of exogenous nano-silicon on salt stress damage of rice seedlings. Int J Mol Sci. 2025;26:85. <https://doi.org/10.3390/ijms26010085>.
 85. Zhu YX, Gong HJ, Yin JL. Role of silicon in mediating salt tolerance in plants: A review. Plants. 2019;8:147. <https://doi.org/10.3390/plants8060147>.
 86. Kumar S, Li G, Yang J, Huang X, Ji Q, Liu Z, Hou H. Effect of salt stress on growth, physiological parameters, and ionic concentration of water dropwort (*Oenanthe javanica*) cultivars. Front Plant Sci. 2021;12:660409. <https://doi.org/10.3389/fpls.2021.660409>.
 87. Ayaz M, Varol N, Yolcu S, Pelvan A, Kaya U, Aydogdu E, Bor M, Özdemir F, Türkkan I. Three (Turkish) Olive cultivars display contrasting salt stress coping mechanisms under high salinity. Trees. 2021;35:1283–98. <https://doi.org/10.1007/s00468-021-02115-w>.
 88. Rahnesan Z, Nasibi F, Moghadam AA. Effects of salinity stress on some growth, physiological, biochemical parameters and nutrients in two pistachio (*Pistacia vera* L.) rootstocks. J Plant Interact. 2018;13(1):73–82. <https://doi.org/10.1080/17429145.2018.1424355>.
 89. Singh A, Prakash J, Srivastav M, Singh SK, Awasthi OP, Singh AK, Sharma DK. Physiological and biochemical responses of citrus rootstocks under salinity stress. Indian J Hort. 2014;71(2):162–7.
 90. Saeidinia M, Beiranvand F, Mumivand H, Mousavi SH. The effect of the salinity stress on the yield, morphological characteristics, essential oil and RWC of *Satureja hortensis* (case study: Khoramabad, Iran). J Drought Clim Change Res. 2023;1(1):97–108. <https://doi.org/10.22077/jdc.2023.6152.1017>.
 91. Sharma J, Verma S, Sharma A. Importance of silicon in combating a variety of stresses in plants: A review. J Nat Appl Sci. 2022;14:607–30. <https://doi.org/10.31018/jans.v14i2.3426>.
 92. Wang M, Gao L, Dong S, Sun Y, Shen Q, Guo S. Role of silicon on plant–pathogen interactions. Front Plant Sci. 2017;8:701. <https://doi.org/10.3389/fpls.2017.00701>.
 93. Liu P, Yin L, Wang S, Zhang M, Deng X, Zhang S. Enhanced root hydraulic conductance by Aquaporin regulation accounts for silicon alleviated salt induced osmotic stress in *Sorghum bicolor* L. Environ Exp Bot. 2015;111:42–51. <https://doi.org/10.1016/j.envexpbot.2014.10.006>.
 94. Zahra N, Al Hinai MS, Hafeez MB, Rehman A, Wahid A, Siddique KHM, Farooq M. Regulation of photosynthesis under salt stress and associated tolerance mechanisms. Plant Physiol Biochem. 2022;178:55–69. <https://doi.org/10.1016/j.plaphy.2022.03.003>.
 95. Hameed A, Ahmed MZ, Hussain T, Aziz I, Ahmad N, Gul B, Nielsen BL. Effects of salinity stress on chloroplast structure and function. Cells. 2021;10(8). <https://doi.org/10.3390/cells10082023>.
 96. Hura T, Szezyk-Taranek B, Hura K, Nowak K, Pawłowska B. Physiological responses of *Rosa rubiginosa* to saline environment. Water Air Soil Pollut. 2017;228:1–11. <https://doi.org/10.1007/s11270-017-3263-2>.
 97. Rathinapriya P, Pandian S, Rakkammal K, Balasangeetha M, Alexpandi R, Satish L, Rameshkumar R, Ramesh M. The protective effects of polyamines on salinity stress tolerance in Foxtail millet (*Setaria Italica* L.), an important C4 model crop. Physiol Mol Biol Plants. 2020;26(9):1815–29. <https://doi.org/10.1007/s12298-020-00869-0>.
 98. Gill SS, Tuteja N. Reactive oxygen species and antioxidant machinery in abiotic stress tolerance in crop plants. Plant Physiol Biochem. 2010;48:909–93. <https://doi.org/10.1016/j.plaphy.2010.08.016>.
 99. Ji X, Tang J, Fan W, Li B, Bai Y, He J, Pei D, Zhang J. Phenotypic differences and physiological responses of salt resistance of walnut with four rootstock types. Plants. 2022;11:1557. <https://doi.org/10.3390/plants11121557>.
 100. Mahmoud LM, Shalan AM, El-Boray MS, Vincent CI, El-Kady ME, Grosser JW, Dutt M. Application of silicon nanoparticles enhances oxidative stress tolerance in salt stressed 'Valencia' sweet orange plants. Sci Hort. 2022;295:110856. <https://doi.org/10.1016/j.scienta.2021.110856>.

101. El Moukhtari A, Carol P, Mouradi M, Savoure A, Farissi M. Silicon improves physiological, biochemical, and morphological adaptations of alfalfa (*Medicago sativa* L.) during salinity stress. *Symbiosis*. 2021;85:305–24. <https://doi.org/10.1007/s13199-021-00814-z>.
102. Ebeed HT, Ahmed HS, Hassan NM. Silicon transporters in plants: unravelling the molecular Nexus with sodium and potassium transporters under salinity stress. *Plant Gene*. 2024;38:100453. <https://doi.org/10.1016/j.plgene.2024.100453>.
103. Soundararajan P, Manivannan A, Ko CH, Jeong BR. Silicon enhanced redox homeostasis and protein expression to mitigate the salinity stress in *Rosa hybrida* 'rock fire'. *J Plant Growth Regul*. 2018;37:16–34. <https://doi.org/10.1007/s00344-017-9705-7>.
104. Shen Z, Pu X, Wang S, Dong X, Cheng X, Cheng M. Silicon improves ion homeostasis and growth of liquorice under salt stress by reducing plant Na⁺ uptake. *Sci Rep*. 2022;12:5089. <https://doi.org/10.1038/s41598-022-05061-8>.
105. Abdelaal KA, Mazrou YS, Hafez YM. Silicon foliar application mitigates salt stress in sweet pepper plants by enhancing water status, photosynthesis, antioxidant enzyme activity and fruit yield. *Plants*. 2020;9(6):733. <https://doi.org/10.3390/plants9060733>.
106. Rad PB, Roozban MR, Karimi S, Ghahremani R, Vahdati K. Osmolyte accumulation and sodium compartmentation has a key role in salinity tolerance of pistachios rootstocks. *Agriculture*. 2021;11:708. <https://doi.org/10.3390/agriculture11080708>.
107. Acharya BR, Sandhu D, Dueñas C. Morphological, physiological, biochemical, and transcriptome studies reveal the importance of transporters and stress signaling pathways during salinity stress in *Prunus*. *Sci Rep*. 2022;12:1274. <https://doi.org/10.1038/s41598-022-05202-1>.
108. Tabatabaei S. Effects of salinity and N on the growth, photosynthesis and N status of Olive (*Olea Europaea* L.) trees. *Sci Hortic*. 2016;108:432–8. <https://doi.org/10.1016/j.scienta.2006.02.016>.
109. Zrig A, Ben Mohamed H, Tounekti T, Khemira H, Serrano M, Valero D, Vadel AM. Effect of rootstock on salinity tolerance of sweet almond (cv. Mazzetto). *S Afr J Bot*. 2016;102:50–9. <https://doi.org/10.1016/j.sajb.2015.09.001>.
110. Ferrández-Gómez BD, Jordá- Cerdán M, Sánchez-Sánchez A. Enhancing salt stress tolerance in tomato (*solanum lycopersicum* L.) through silicon application in roots. *Plants*. 2024;13:1415. <https://doi.org/10.3390/plants13101415>.
111. Sartori Camargo M, Jonas Baltieri G, Luiz Santos H, Rodrigues Alves Carnietto M, Rodrigues dos Reis A, Claudia Pacheco A, de Almeida Silva M. Silicon fertilization enhances photosynthetic activity and sugar metabolism in sugarcane cultivars under water deficit at the ripening phase. *Silicon*. 2023;15:3021–33. <https://doi.org/10.1007/s12633-022-02236-y>.
112. Gao H, Yu W, Yang X, Liang J, Sun X, Sun M, Xiao Y, Peng F. Silicon enhances the drought resistance of Peach seedlings by regulating hormone, amino acid, and sugar metabolism. *BMC Plant Biol*. 2022;22:422. <https://doi.org/10.1186/s12870-022-03785-5>.
113. Hasanuzzaman M, Raihan MRH, Nowroz F, Fujita M. Insight into the mechanism of salt-induced oxidative stress tolerance in soybean by the application of *Bacillus subtilis*: coordinated actions of osmoregulation, ion homeostasis, antioxidant defense, and Methylglyoxal detoxification. *Antioxidants*. 2022;11:1856. <https://doi.org/10.3390/antiox11101856>.
114. Figueroa-Soto CG, Valenzuela-Soto EM. Glycine betaine rather than acting only as an osmolyte also plays a role as regulator in cellular metabolism. *Biochim*. 2018;147:89–97. <https://doi.org/10.1016/j.biochi.2018.01.002>.
115. Shahid MA, Balal RM, Khan N, Simón-Grao S, Alfosea-Simón M, Cámara-Zapata JM, García-Sánchez F. Rootstocks influence the salt tolerance of Kinnow Mandarin trees by altering the antioxidant defense system, osmolyte concentration, and toxic ion accumulation. *Sci Hortic*. 2019;250:1–11. <https://doi.org/10.1016/j.scienta.2019.02.028>.
116. Sorkheh K, Shiran B, Rouhi V, Khodambashi M, Sofo A. Salt stress induction of some key antioxidant enzymes and metabolites in eight Iranian wild almond species. *Acta Physiol Plant*. 2012;34:203–13. <https://doi.org/10.1007/s11738-011-0819-4>.
117. Dou Z, Feng H, Zhang H, Abdelghany AE, Zhang F, Li Z, Fan J. Silicon application mitigated the adverse effects of salt stress and deficit irrigation on drip-irrigated greenhouse tomato. *Agric Water Manag*. 2023;289(1):108526. <https://doi.org/10.1016/j.agwat.2023.108526>.
118. Tripathi DK, Vishwakarma K, Singh VP, Prakash V, Sharma S, Muneer S, Nikolic M, Deshmukh R, Vaculik M, Corpas FJ. Silicon crosstalk with reactive oxygen species, phytohormones and other signaling molecules. *J Hazard Mater*. 2021;408(15):124820. <https://doi.org/10.1016/j.jhazmat.2020.124820>.
119. Kesawat MS, Satheesh N, Kherawat BS, Kumar A, Kim HU, Chung SM, Kumar M. Regulation of reactive oxygen species during salt stress in plants and their crosstalk with other signaling molecules- current perspectives and future directions. *Plants*. 2023;12(4):864. <https://doi.org/10.3390/plants12040864>.
120. Hatami E, Shokouhian AA, Ghanbari AR, Naseri L. Investigation the effect of humic acid on morphophysiological and biochemical characteristics of almond rootstocks under salinity stress. *Iran J Hortic Sci*. 2020;3(51):523–36.
121. Al Murad M, Khan AL, Muneer S. Silicon in horticultural crops: cross-talk, signaling, and tolerance mechanism under salinity stress. *Plants*. 2020;9:460. <https://doi.org/10.3390/plants9040460>.
122. Yeşildirek YV, Arkan B, Çelik H, Premkumar A, Özden S, Turgut Kara N. Role of silicon in mediating salt stress responses in *Arabidopsis* methylation mutants. *J Soil Sci Plant Nutr*. 2024;24:4471–82. <https://doi.org/10.1007/s42729-024-01848-0>.
123. Mousavi SAA, Roosta HR, Esmailizadeh M, Eshghi S. Silicon and selenium supplementations modulate antioxidant systems and mineral nutrition to mitigate salinity-alkalinity stresses in cucumber (*Cucumis sativus* L.) plants under hydroponic conditions. *J Plant Process Function*. 2022;10(46):41–9. <https://doi.org/10.1007/s10077-022-00092-7>.
124. Muneer S, Jeong BR. Proteomic analysis of salt-stress responsive proteins in roots of tomato (*Lycopersicon esculentum* L.) plants towards silicon efficiency. *Plant Growth Regul*. 2015;77(2):133–46. <https://doi.org/10.1007/s10725-015-045-y>.
125. Delatorre-herrera J, Ruiz KB, Pinto M. The importance of non-diffusional factors in determining photosynthesis of two contrasting Quinoa ecotypes (*Chenopodium Quinoa* Willd.) subjected to salinity conditions. *Plants*. 2021;10(5):927. <https://doi.org/10.3390/plants10050927>.
126. Huang H, Ullah F, Zhou DX, Yi M, Zhao Y. Mechanisms of ROS regulation of plant development and stress responses. *Front Plant Sci*. 2019;10:800. <https://doi.org/10.3389/fpls.2019.00800>.
127. He W, Yan K, Zhang Y, Bian L, Mei H, Han G. Contrasting photosynthesis, photoinhibition and oxidative damage in honeysuckle (*Lonicera Japonica* Thunb.) under iso-osmotic salt and drought stresses. *Environ Exp Bot*. 2021;182:104313. <https://doi.org/10.1016/j.envexpbot.2020.104313>.
128. Gulzar S, Hussain T, Gul B, Hameed A. Photosynthetic adaptations and oxidative stress tolerance in halophytes from warm subtropical region. In: Grigore MN, editor. *Handbook of halophytes*. Cham. DOI: Springer; 2021. https://doi.org/10.1007/978-3-030-57635-6_52.
129. Wang X, Chen Z, Sui N. Sensitivity and responses of chloroplasts to salt stress in plants. *Front Plant Sci*. 2024;15:1374086. <https://doi.org/10.3389/fpls.2024.1374086>.
130. Sandhu D, Kaundal A, Acharya BR, Forest T, Pudusseri MV, Liu X, Ferreira JFS, Suarez DL. Linking diverse salinity responses of 14 almond rootstocks with physiological, biochemical, and genetic determinants. *Sci Rep*. 2020;10(1):1–13. <https://doi.org/10.1038/s41598-020-78036-4>.
131. Liang Y, Liu H, Fu Y, Li P, Li S, Gao Y. Regulatory effects of silicon nanoparticles on the growth and photosynthesis of cotton seedlings under salt and low-temperature dual stress. *BMC Plant Biol*. 2023;23:504. <https://doi.org/10.1186/s12870-023-04509-z>.
132. Sharipova G, Ivanov R, Veselov D, Akhiyarova G, Seldimirova O, Galin I. Effect of salinity on stomatal conductance, leaf hydraulic conductance, HvPIP2 Aquaporin, and abscisic acid abundance in barley leaf cells. *Int J Mol Sci*. 2022;1–9. <https://doi.org/10.3390/ijms232214282>.
133. Rastogi A, Yadav S, Hussain S, Kataria S, Hajjhashemi S, Kumari P, Yang X, Bres-tic M. Does silicon really matter for the photosynthetic machinery in plants? *Plant Physiol Biochem*. 2021;169:40–8. <https://doi.org/10.1016/j.plaphy.2021.11.004>.
134. Farouk S, Al-Huqail AA. Sustainable Biochar and/or melatonin improve salinity tolerance in borage plants by modulating osmotic adjustment, antioxidants, and ion homeostasis. *Plants*. 2022;11(6):765. <https://doi.org/10.3390/plants11060765>.
135. Kaur H, Hussain SJ, Kaur G, Poor P, Alamri S, Siddiqui MH, Khan MIR. Salicylic acid improves nitrogen fixation, growth, yield and antioxidant defense mechanisms in Chickpea genotypes under salt stress. *J Plant Growth Regul*. 2022;41(5):2034–47. <https://doi.org/10.1007/s00344-022-10592-7>.
136. Blumwald E. Sodium transport and salt tolerance in plants. *Curr Opin Cell Biol*. 2000;12(4):431–4. [https://doi.org/10.1016/s0955-0674\(00\)00112-5](https://doi.org/10.1016/s0955-0674(00)00112-5).
137. Parida AK, Das AB. Salt tolerance and salinity effects on plants: A review. *Ecotoxic Environ Saf*. 2005;60(3):324–49. <https://doi.org/10.1016/j.jecoen.2004.06.010>.
138. Mita K, Sumikama T, Iwamoto M, Matsuki Y, Shigemori K, Oiki S. Conductance selectivity of Na⁺ across the K⁺ channel via Na⁺ trapped in a tortuous trajectory. *Proc Natl Acad Sci USA*. 2021;118(12):e2017168118. <https://doi.org/10.1073/pnas.2017168118>.

139. Lux A, Lukacova Z, Vaculik M, Svubova R, Kohanova J, Soukup M, Martinka M, Bokor B. Silicification of root tissues. *Plants*. 2020;9(1):111. <https://doi.org/10.3390/plants9010111>.
140. Ma JF, Tamai K, Yamaji N, Mitani N, Konishi S, Katsuhara M, Ishiguro Murata Y, Yano M. A silicon transporter in rice. *Nature*. 2006;440:688–91. <https://doi.org/10.1038/nature04590>.
141. Guerriero G, Hausman JF, Legay S. Silicon and the plant extracellular matrix. *Front Plant Sci*. 2016;7:463. <https://doi.org/10.3389/fpls.2016.00463>.
142. Fleck AT, Nye T, Repenning C, Stahl F, Zahn M, Schenk MK. Silicon enhances suberization and lignification in roots of rice (*Oryza sativa*). *J Exp Bot*. 2011;62(6): 2001–11. <https://doi.org/10.1093/jxb/erq392>. Epub 2010 Dec 13.
143. Shao Y, Cheng Y, Pang H, Chang M, He F, Wang M, Drakakaki G. Investigation of salt tolerance mechanisms across a root developmental gradient in almond rootstocks. *Front Plant Sci*. 2021;11:595055. <https://doi.org/10.3389/fpls.2020.595055>.
144. Kaundal A, Sandhu D, Duenas M, Ferreira JFS. Expression of the high-affinity K⁺ transporter 1 (*PpHKT1*) gene from almond rootstock 'nemaguard' improved salt tolerance of Transgenic arabidopsis. *PLoS ONE*. 2019;14(3):e0214473. <https://doi.org/10.1371/journal.pone.0214473>. eCollection 2019.
145. Gupta B, Huang B. Mechanism of salinity tolerance in plants: physiological, biochemical, and molecular characterization. *Int J Genomics*. 2014;701596. <https://doi.org/10.1155/2014/701596>.
146. Munns R, Tester M. Mechanisms of salinity tolerance. *Annu Rev Plant Biol*. 2008;59:651–81. <https://doi.org/10.1146/annurev.arplant.59.032607.092911>.
147. Li Y, Niu W, Cao X, Wang J, Zhang M, Duan X, Zhang Z. Effect of soil aeration on root morphology and photosynthetic characteristics of potted tomato plants (*Solanum lycopersicum*) at different NaCl salinity levels. *BMC Plant Biol*. 2021;19:331. <https://doi.org/10.1186/s12870-019-1927-3>.

Publisher's note

Springer Nature remains neutral with regard to jurisdictional claims in published maps and institutional affiliations.